

**Kondo effect and STM spectra through ferromagnetic nanoclusters**Gregory A. Fiete,<sup>1</sup> Gergely Zarand,<sup>1</sup> Bertrand I. Halperin,<sup>1</sup> and Yuval Oreg<sup>2</sup><sup>1</sup>*Department of Physics, Harvard University, Cambridge, Massachusetts 02138*<sup>2</sup>*Weizmann Institute of Science, P.O. Box 26, Rehovot 76100, Israel*

(Received 13 December 2001; revised manuscript received 11 April 2002; published 22 July 2002)

Motivated by recent scanning tunneling microscope (STM) experiments on cobalt clusters adsorbed on single-wall metallic nanotubes [Odom *et al.*, *Science* **290**, 1549 (2000)], we study theoretically the size dependence of STM spectra and spin-flip scattering of electrons from finite size ferromagnetic clusters adsorbed on metallic surfaces. We study two models of nanometer size ferromagnets. (i) An itinerant model with delocalized  $s$ ,  $p$ , and  $d$  electrons and (ii) a local moment model with both localized  $d$ -level spins and delocalized cluster electrons. The effective exchange coupling between the spin of the cluster and the conduction electrons of the metallic substrate depends on the specific details of the single-particle density of states on the cluster. The calculated Kondo coupling is inversely proportional to the total spin of the ferromagnetic cluster in both models and thus the Kondo temperature is rapidly suppressed as the size of the cluster increases. Mesoscopic fluctuations in the charging energies and magnetization of nanoclusters can lead to large fluctuations in the Kondo temperatures and a very asymmetric voltage dependence of the STM spectra. We compare our results to the experiments.

DOI: 10.1103/PhysRevB.66.024431

PACS number(s): 73.22.-f, 72.10.Fk, 73.63.Fg

**I. INTRODUCTION**

Kondo physics<sup>1</sup> has seen a revival in recent years due to an exciting series of new experiments on mesoscopic<sup>2,3</sup> and nanoscale<sup>4-7</sup> systems, which has enabled a more thorough and controlled study of the basic problem of a local moment interacting with a sea of conduction electrons. It is now possible, for example, in quantum dots, to tune the Kondo temperature,  $T_K$ , with externally applied gate voltages<sup>2,3,6</sup> or, with the scanning tunneling microscope (STM), to study the Kondo effect at single magnetic impurities on metallic surfaces.<sup>4,5</sup> The superb spatial resolution of the STM permits unprecedented direct local spectroscopic detail of Kondo impurities.

Recent low-temperature ( $\sim 4$  K) STM experiments<sup>7</sup> have probed the spectroscopy of isolated nanometer and subnanometer ferromagnetic (Co) clusters on metallic single-walled carbon nanotubes.<sup>8</sup> The tunneling spectrum of these small ferromagnetic clusters exhibited several interesting features—most notably Kondo effect in subnanometer diameter clusters and well resolved discrete level spacing in nanometer size clusters. Both subnanometer and nanometer size clusters exhibited a Coulomb charging gap in the spectrum near zero bias. The Kondo effect in the subnanometer size clusters appeared in the spectrum as a Fano-like sharp peak<sup>9,10</sup> with a half-width  $\sim 15$  meV ( $T_K \sim 80$  K) at 4 K. This peak was not present at 100 K, presumably due to thermal destruction of the Kondo resonance.

The goal of this paper is to present a theoretical framework to study the spin-flip scattering of conduction electrons from finite-size ferromagnetic clusters adsorbed on metallic surfaces. In particular, we are interested in understanding some of the *size-dependent features* observed in the tunneling spectrum. We focus on how the Kondo Effect, the level spacing, and the level widths depend on the size of the cluster.

Cluster ferromagnetism may be described by two alternate models.

(i) In the experiments of Odom *et al.*<sup>7</sup> magnetism of the cluster is most likely *itinerant* in nature as bulk Co is an itinerant band ferromagnet. The basic physics of itinerant clusters is captured in the model of Refs. 11 and 12 (see Sec. II).

(ii) In some other cases, however, including the case of many semiconducting ferromagnets<sup>13</sup> and rare-earth materials, ferromagnetism is better described in terms of *local moments* that couple ferromagnetically or antiferromagnetically to the cluster conduction electrons (holes).

This motivated us to introduce another exactly solvable model, where  $d$ -electrons produce highly localized magnetic moments. While the excitation spectrum of the two models turns out to be very similar, the way they couple to the metallic substrate is rather different. The most appropriate model to use in a given physical situation depends on the material that composes the nanoparticle and whether it is more appropriate to think of the magnetism of the particle as due to localized moments or itinerant electrons that, although free to move about, are nevertheless polarized strongly enough to give a net spin to the cluster.

We make several assumptions during our computations. We assume the clusters to have between, say, eight and forty atoms and that they are large enough that bulk properties, such as the magnetization per atom, are not changed substantially due to their finite size. Furthermore, we assume that the single-particle states on the island are of extended character, and therefore the single-particle level spacing decreases as  $\sim 1/N_A$  with an increasing number of cluster atoms,  $N_A$ . We also assume that the ferromagnetic spin splitting  $\Delta_s$  of the extended states on the island is much larger than the single-particle level spacing and is approximately independent of the size of the cluster. Thus the total spin of the cluster is rather large and is roughly proportional to  $\sim N_A \gg 1$ .

Depending on the strength of the electron tunneling be-

tween the metal and the cluster we may distinguish two regimes: weak and strong. For weak tunneling we derive an effective Kondo Hamiltonian in second-order perturbation theory in the tunneling. In this regime we find that at very low energy scales the cluster behaves most similarly to a quantum dot with a single unpaired electron. However, ferromagnetic interactions induce a large spin on the cluster and at the same time *reduce* the value of the effective exchange coupling between the spin of the cluster and the electrons in the metal.

The sign of the exchange coupling depends on the specific details of the band structure on the nanoparticle. For a Co cluster, in particular, the itinerant model gives a tendency for *antiferromagnetic* coupling, and possibly produces a Kondo effect. However, the Kondo temperature  $T_K$ , decreases very fast with increasing cluster sizes, and therefore the Kondo effect can be observed only for very small clusters.

The effective couplings we obtain,  $J^{\text{eff}}$ , turn out to be in general  $M \times M$  matrices describing spin-flip scattering among the  $M$  conduction band orbital modes that couple to the cluster ( $M=4$  for metallic nanotubes.<sup>14</sup>) Therefore we expect that a series of Kondo effects takes place at Kondo temperatures corresponding to the antiferromagnetic eigenvalues of  $J^{\text{eff}}$ . The total spin of the impurity,  $S_T$  gets successively screened at each Kondo temperature as the temperature is lowered:  $S_T \rightarrow S_T - 1/2 \rightarrow S_T - 1 \dots$ . For a nanotube this compensation can never be complete<sup>15</sup> for any spin greater than 2 since there are only four channels available for screening.<sup>14</sup> The degeneracy of the remaining unscreened spin will ultimately be lifted by magnetic anisotropy induced by spin-orbit coupling.<sup>16</sup>

To make closer contact with the experiments of Odom *et al.*<sup>7</sup> we compute the STM tunneling spectrum using the itinerant model. The simultaneous observation of the Coulomb gap and the discrete levels, whose widths almost equal the level spacing, suggest that the clusters investigated are in the intermediate tunneling regime. Nevertheless, carrying out perturbative calculations in the weak tunneling limit, we are able to reproduce the essential features of the STM spectrum *above* the the Coulomb charging energy. We find that small fluctuations in the charging energies can give rise to very asymmetrical STM spectra.

From the STM spectra of the clusters at higher voltages, we can crudely estimate the Kondo temperature,  $T_K$ , of a small Co cluster of the size that exhibited a Kondo effect in Ref. 7. However, our estimates tend to give a  $T_K$  that is too small. We find that typical mesoscopic fluctuations in the charging energies of a ferromagnetic cluster can considerably increase the Kondo temperature, however, they do not account for the difference between our theoretical estimates and the experimentally observed  $T_K$ .<sup>7</sup> Nevertheless, the fact that some small Co clusters exhibit Kondo effect while others do not, indicates that these mesoscopic fluctuations may indeed play an important role in determining  $T_K$ . Since  $T_K$  depends exponentially on  $J^{\text{eff}}$ , relatively small changes in the latter can induce large variations of  $T_K$ .

This paper is organized as follows. In Sec. II we introduce the itinerant model of nanoscale ferromagnets. In Sec. III we study the spin-flip scattering of conduction electrons from an

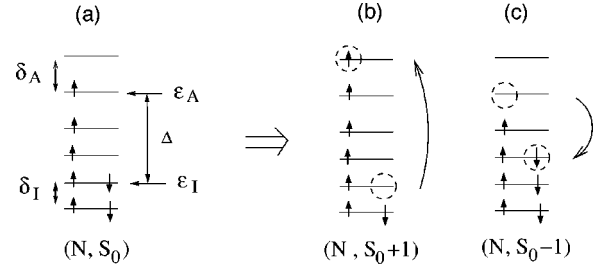


FIG. 1. Spin excitations of a ferromagnetic nanoparticle. For the precise definition of  $\epsilon_{A/I}$ ,  $\delta_{A/I}$ , and  $\Delta_s$  see text. (a) The fully polarized ground state. (b) and (c), lowest lying particle-hole excitations having energy  $\sim \delta_{A/I}$ .

itinerant cluster using second-order perturbation theory in the cluster-substrate tunneling, and we derive a general expression for the matrix of Kondo couplings,  $J^{\text{eff}}$ . In Sec. IV we make contact to the experiments of Odom *et al.*<sup>7</sup> by calculating in a simple approximation the STM tunneling spectrum of a ferromagnetic Co cluster on a metallic substrate in the limit of weak tunneling. In Sec. V we introduce a local moment model for ferromagnetism and show how to compute the effective interaction  $J^{\text{eff}}$  in this case. In Sec. VI we discuss in detail the connection between our work and recent experiments. Finally, in Sec. VII we present our conclusions.

## II. ITINERANT FERROMAGNETIC CLUSTER MODEL

An itinerant mean-field model of a magnetic nanoparticle was first proposed by Canali and MacDonald<sup>11</sup> and later extended by Kleff *et al.*<sup>12</sup> to explain the dense spectrum in tunneling measurements of nanometer size Co particles.<sup>17</sup> The basic Hamiltonian is

$$\hat{H}_{\text{cluster}} = \sum_{j,\sigma} \epsilon_j c_{j\sigma}^\dagger c_{j\sigma} - \frac{1}{2} \frac{U}{N_A} \vec{S} \cdot \vec{S} + \frac{E_C}{2} (\hat{N} - n_g)^2, \quad (1)$$

where  $c_{j\sigma}^\dagger$  ( $c_{j\sigma}$ ) creates (destroys) an electron with spin  $\sigma$  at the  $j$ th energy level of the cluster with kinetic energy  $\epsilon_j$  (see Fig. 1). The first term in Eq. (1) represents the kinetic energy of the hybridized  $s$ -,  $p$ -, and  $d$ -band electrons. The parameter  $U > 0$  is the effective ferromagnetic exchange interaction on the cluster,  $N_A$  is the number of atoms that constitute the cluster, and

$$\vec{S} = \sum_j \frac{1}{2} \sum_{\alpha,\alpha'} c_{j\alpha}^\dagger \vec{\sigma}_{\alpha\alpha'} c_{j\alpha'} \quad (2)$$

is the total spin of the cluster. The second term in Eq. (1) corresponds to ferromagnetic exchange on the cluster. It gives rise to a spontaneous polarization of the cluster by making spin alignment of different levels energetically favorable. Finally, the last term describes the charging of the cluster with  $E_C$  the Coulomb charging energy,  $\hat{N} = \sum_{j,\sigma} \hat{n}_{j\sigma}$  the total number of electrons on the cluster, and  $n_g$  a dimensionless gate voltage that determines the number of electrons in the ground state.<sup>18</sup>

Throughout this paper we are neglecting fluctuations in the level spacing. In a *real* nanoparticle, the level spacing

between the  $j$ th and  $(j+1)$ th energy level can be written as  $\delta_j = \langle \delta_j \rangle + \eta_j$ , where  $\langle \delta_j \rangle$  is the level spacing corresponding to the bulk energy-dependent density of states,  $\langle \delta_j \rangle \sim 1/\rho(\epsilon_j)$ , and  $\eta_j$  ( $\langle \eta_j \rangle = 0$ ) is a fluctuating part due to shape irregularities in the nanoparticle. In this paper we take  $\eta_j \equiv 0$ , corresponding to an infinitely strong level repulsion.

The advantage of this model is that  $S^z$ ,  $S^2$ , and  $n_j$  are conserved quantities and therefore the Hamiltonian in Eq. (1) can be diagonalized exactly. In the more general situation a magnetic anisotropy term should be added to the Hamiltonian. Nevertheless, for the experimentally investigated clusters this anisotropy is estimated to be much less than the width of the Kondo resonance observed, and therefore it can be neglected.<sup>19</sup>

The ground state can be explicitly constructed,<sup>12</sup>

$$|S_0, S^z = S_0\rangle_G^N = \prod_{j=1}^{n_\uparrow} c_{j\uparrow}^\dagger \prod_{j=1}^{n_\downarrow} c_{j\downarrow} |vac\rangle, \quad (3)$$

with  $S_0$  and  $N$  the spin and particle number in the ground state. The remaining states within the ground-state multiplet may be explicitly constructed using the lowering operator,

$$|S_0, S^z\rangle_G^N = \sqrt{\frac{(S_0 + S^z)!}{(2S_0)!(S_0 - S^z)!}} (S^-)^{(S_0 - S^z)} |S_0, S_0\rangle_G^N. \quad (4)$$

In itinerant ferromagnets there is an approximate rigid band splitting between spin-up and spin-down electron density of states.<sup>20</sup> Throughout this paper, we will assume that our clusters are large enough that the band splitting energy,  $\Delta_s$ , is well approximated by the bulk value of the specific material we are considering. In our model  $\Delta_s$  can be defined as the energy difference between the highest occupied spin-up level,  $\epsilon_A$ , and the highest occupied spin-down level,  $\epsilon_I$ ,

$$\Delta_s \equiv \epsilon_A - \epsilon_I,$$

and from band-structure calculations it is known to be typically of the order of a few electron volts<sup>20</sup> (see Fig. 1). It can be determined by demanding that the ground state of the ferromagnetic cluster be stable to fluctuations of energy-level occupations with constant particle number, and is related to the interaction parameter  $U$  as<sup>11</sup>

$$U = \frac{N_A}{S_0} \Delta_s + d_0, \quad (5)$$

where  $d_0$  is a small quantity that scales as  $1/N_A$ , while the first term is roughly independent of the cluster size, since  $S_0 \sim N_A$ . Using Eq. (5), one can estimate the energy cost of a particle-hole excitation [see Figs. 1(b) and 1(c)]. This turns out to be of the order of the level spacing ( $\propto 1/N_A$ ) (and *not* the exchange splitting  $\Delta_s$ ),

$$\delta E(S_0 \pm 1, N) \equiv \min\{E_{\text{excited}}(S_0 \pm 1, N) - E_G\} \sim \delta_A, \delta_I, \quad (6)$$

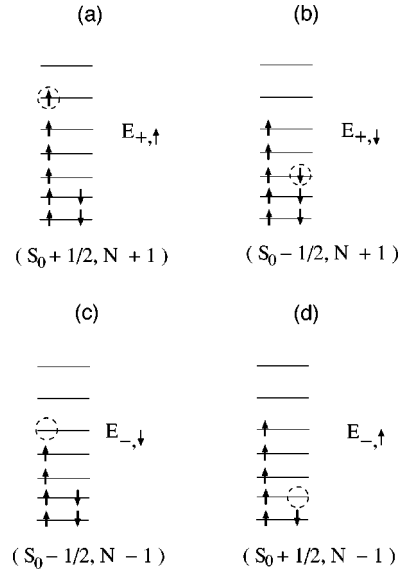


FIG. 2. Charging excitations of a ferromagnetic particle. Circles indicate particles added to (removed from) the ground state. (a), (b): lowest energy state for adding a majority (minority) electron to the cluster. (c), (d): lowest energy state for adding a majority (minority) hole to the cluster.

where  $E_G$  denotes the ground-state energy, and  $\delta_A$  ( $\delta_I$ ) is the level spacing near  $\epsilon_A$  ( $\epsilon_I$ ). If  $U$  is large enough to fully polarize the cluster, the energy scales outlined above may change.<sup>21</sup>

The minimum cost of adding a particle or a hole to the cluster can be defined as

$$\delta E_{\pm, \sigma} \equiv \min\{E(N \pm 1, S_0 + \sigma/2) - E_G\}, \quad (7)$$

where the minimum is over all possible excited states. To determine  $\delta E_{\pm, \sigma}$  we consider processes like those in Fig. 2. These energies can be estimated as

$$\delta E_{+, \uparrow} \approx \bar{\epsilon} + E_C^+ + \left( \delta_A - \frac{1}{2} \frac{S_0}{N_A} d_0 - \frac{3}{8} \frac{\Delta_s}{S_0} \right), \quad (8)$$

$$\delta E_{+, \downarrow} \approx \bar{\epsilon} + E_C^+ + \left( \delta_I + \frac{1}{2} \frac{S_0}{N_A} d_0 + \frac{1}{8} \frac{\Delta_s}{S_0} \right), \quad (9)$$

$$\delta E_{-, \uparrow} \approx \bar{\epsilon} + E_C^- - \left( \frac{1}{2} \frac{S_0}{N_A} d_0 + \frac{3}{8} \frac{\Delta_s}{S_0} \right), \quad (10)$$

$$\delta E_{-, \downarrow} \approx \bar{\epsilon} + E_C^- + \left( \frac{1}{2} \frac{S_0}{N_A} d_0 + \frac{1}{8} \frac{\Delta_s}{S_0} \right), \quad (11)$$

where the corrections scale as  $O(1/N_A^2)$ , and  $E_C^\pm$  denote the charging energies in the limit of vanishing ferromagnetic coupling and an infinitely dense single-particle spectrum,

$$E_C^\pm \equiv E_C \left( \frac{1}{2} \pm (N - n_g) \right). \quad (12)$$

The parameter  $\bar{\epsilon} \equiv (\epsilon_A + \epsilon_I)/2$  in Eq. (8) can be absorbed into the definition of  $n_g$ , and we will set it to zero in what follows.

The last terms in Eqs. (8)–(11), proportional to  $\Delta_s/S_0$ , are specific to the mean-field model discussed here and have little physical meaning. Their effect can be fully taken into account by renormalizing the “chemical potential”  $\bar{\epsilon}$  and the mesoscopic parameter  $d_0$ , and they therefore do not modify our results.

Using a stability analysis similar to the previous one it is a trivial matter to show that typically

$$\delta E_{\pm, \sigma} \sim E_C/2. \quad (13)$$

For later purposes it is also useful to have excitation energies of particles and holes added to *any* level defined,  $\delta E_{\pm, \sigma}^j(N \pm 1, S_0 + \sigma/2)$ . For example, increasing the total spin by adding an electron to the  $j$ th unoccupied level rather than the one immediately above  $\epsilon_A$  gives,

$$\delta E_{+, \uparrow}^j \equiv \epsilon_j - (\epsilon_A + \delta_A) + \delta E_{+, \uparrow}. \quad (14)$$

Removing an electron from level  $j$  below  $\epsilon_I$  so that the total spin increases gives

$$\delta E_{-, \uparrow}^j \equiv \epsilon_I - \epsilon_j + \delta E_{-, \uparrow}. \quad (15)$$

It is important to point out that in our model all effects of mesoscopic fluctuations have been put into the quantities  $E_C$ ,  $d_0$ , and  $n_g$ . All other quantities of the itinerant model are specified by the bulk band structure and the number of atoms,  $N_A$ , in a given nanocluster.

### III. WEAK TUNNELING BETWEEN A FERROMAGNETIC CLUSTER AND A METAL

#### A. General expression

A finite-size ferromagnetic cluster can scatter electrons between different orbital channels in the substrate and flip their spin while doing so. If the spin-orbit coupling is sufficiently weak then SU(2) symmetry in the spin sector implies that the low-energy effective interaction between the cluster spin and the electrons takes the form (apart from a potential scattering term)

$$\hat{H}_{\text{Kondo}}^{\text{eff}} = \frac{1}{2} \sum_{k, k'} J^{\mu\nu} \vec{S} \cdot a_{\mu k \alpha}^\dagger \vec{\sigma}_{\alpha \alpha'} a_{\nu k' \alpha'}, \quad (16)$$

where  $J^{\mu\nu}$  is a Hermitian matrix of spin-flip exchange couplings among the various orbital channels, indexed by  $\mu$  and  $\nu$ . (In a one-dimensional system, such as a carbon nanotube,  $\mu$  labels left-going and right-going modes of different symmetries. In an isotropic two or three dimensional host  $\mu$  labels angular momenta about the cluster.) The total spin of the cluster is  $\hat{S}$  and the  $a_{\mu k \alpha}^\dagger$  ( $a_{\mu k \alpha}$ ) are creation (annihilation) operators for conduction electrons of the metal in orbital channel  $\mu$ , wave number  $k$ , and spin  $\alpha$ . A finite-size cluster in an isotropic host will generally scatter electrons among all orbital channels, but in practice  $J^{\mu\nu}$  can be truncated to include a finite number of channels, the largest angular momentum being  $l \sim L/\lambda_F$  where  $L$  is the size of the cluster and  $\lambda_F$  is the Fermi wavelength of the conduction electrons.

In the limit of weak tunneling,  $J^{\mu\nu}$  can be calculated in second-order perturbation theory in the tunneling. The Hamiltonian we consider is  $\hat{H} = \hat{H}_0 + \hat{V}$ , where  $\hat{H}_0 = \hat{H}_{\text{metal}} + \hat{H}_{\text{cluster}}$  and where  $\hat{H}_{\text{metal}} = \sum_{\mu, k, \sigma} \epsilon_{\mu, k} a_{\mu k \sigma}^\dagger a_{\mu k \sigma}$  is the Hamiltonian of the free conduction electrons of the metal and

$$\hat{V} = \sum_{\mu, \sigma, j, k} (V_{\mu}^{j, k} c_{j\sigma}^\dagger a_{\mu k \sigma} + \text{H.c.}), \quad (17)$$

where

$$V_{\mu}^{j, k} \equiv \sum_{n=1}^{N_p} V_n \varphi_j^*(\vec{R}_n) \psi_{\mu, k}(\vec{R}_n), \quad (18)$$

and  $N_p$  is the number of points of electrical contact between the cluster and the metal. The  $\varphi_j(\vec{R}_n)$  are the wave functions of the  $j$ th levels on the cluster at the points of contact  $\vec{R}_n$  and the  $\psi_{\mu, k}(\vec{R}_n)$  are the wave functions of the metal at  $\vec{R}_n$ . The tunneling amplitude  $V_n$  can be estimated with a knowledge of the wave functions near the cluster-metal contact points and the work functions of the cluster and the metal.

We can determine  $J^{\mu\nu}$  by equating

$$\langle f | \hat{H}_{\text{Kondo}}^{\text{eff}} | i \rangle = \sum_n \frac{\langle f | \hat{V} | n \rangle \langle n | \hat{V} | i \rangle}{E_i - E_n}, \quad (19)$$

where  $|i\rangle = |S_0, S^z\rangle_G |v, k_i, \sigma\rangle$  and  $|f\rangle = |S_0, S^{z'}\rangle_G |\mu, k_f, \sigma'\rangle$  denote the initial and final states with energies  $E_i$  and  $E_f$ , respectively, and  $|n\rangle$  stands for all possible intermediate states with energy  $E_n$ ,  $H_0 |n\rangle = E_n |n\rangle$ . Here  $|v, k, \sigma\rangle$  denotes the Fermi sea with an additional electron in the  $\nu$ th channel with momentum  $k$  and spin  $\sigma$ .

The easiest way to determine  $J^{\mu\nu}$  is to focus on purely spin-flip processes to which potential scattering does not contribute, and choose  $S^z = S_0, \sigma = \downarrow$  and  $S^{z'} = S_0 - 1, \sigma' = \uparrow$ , giving  $\langle f | \hat{H}_{\text{Kondo}}^{\text{eff}} | i \rangle = \frac{1}{2} \sqrt{2S_0} J^{\mu\nu}$ . The right-hand side (RHS) of Eq. (19) is evaluated by summing over both states with an extra particle and states with an extra hole in the intermediate state (See Fig. 3). After a rather straightforward computation we find that  $J^{\mu\nu}$  is given by the sum of three contributions,

$$J^{\mu\nu} = J_d^{\mu\nu} + J_s^{\mu\nu} + J_e^{\mu\nu}. \quad (20)$$

The couplings  $J_d^{\mu\nu}$  and  $J_e^{\mu\nu}$  describe the contributions from tunneling processes involving doubly occupied and empty single particle levels,

$$J_d^{\mu\nu} = -\frac{1}{S_0 + 1/2} \sum_{j \leq l} V_{\mu}^{j, k_f} V_{\nu}^{j, k_i} \times \left( \frac{1}{\delta E_{-, \uparrow} + \epsilon_I - \epsilon_j} - \frac{1}{\delta E_{-, \downarrow} + \Delta_s + \epsilon_I - \epsilon_j} \right), \quad (21)$$

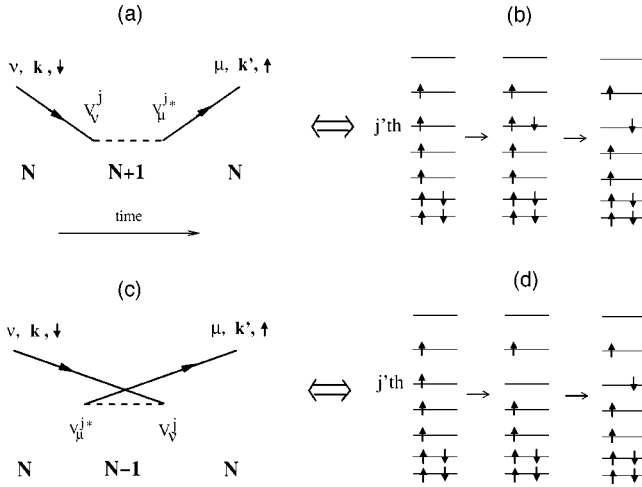


FIG. 3. Kondo scattering from a ferromagnetic cluster. (a) and (c), time ordered diagrams in second order perturbation generating the single-particle contribution Eq. (23) to the effective exchange  $J^{\mu\nu}$ . Solid lines represent the incoming and outgoing electrons while dashed lines denote the intermediate excited state of the nanoparticle. In (a) an electron in state  $|\nu, k, \downarrow\rangle$  hops on the cluster onto level  $j$  and another electron leaves the cluster from level  $j$  with outgoing state  $|\mu, k', \uparrow\rangle$ . In (c) first an electron hops out from level  $j$  into state  $|\mu, k', \uparrow\rangle$  and then the incoming electron hops onto level  $j$ . Level occupation changes are shown in (d).

$$J_e^{\mu\nu} = -\frac{1}{S_0 + 1/2} \sum_{j>A} V_\mu^{j,k_f*} V_\nu^{j,k_i} \times \left( \frac{1}{\delta E_{+,\uparrow} - \epsilon_{A+1} + \epsilon_j} - \frac{1}{\delta E_{+,\downarrow} + \Delta_s - \epsilon_{A+1} + \epsilon_j} \right), \quad (22)$$

and the incoming and outgoing electrons were put at the Fermi energy. Since  $\Delta_s \gg \delta E_{\pm, \sigma}$  both contributions are *ferromagnetic*, i.e., all eigenvalues of  $J_d^{\mu\nu} + J_e^{\mu\nu}$  are negative. To see this let us first neglect the  $k$  dependence of the  $V_\mu^{j,k,s}$ . Then the matrices  $J_a^{\mu\nu}$  ( $a = e, d$ ) can be expressed as a sum,  $J_a^{\mu\nu} = \sum_j P_j^{\mu\nu}$ . Each of these terms is obviously negative semidefinite, i.e., for any vector  $a^\mu$  the product  $a_\mu^* P_j^{\mu\nu} a_\nu$  is negative or zero. As a consequence,  $J_e^{\mu\nu}$  and  $J_d^{\mu\nu}$  are also negative semidefinite, i.e., in a diagonal basis all their eigenvalues are negative or zero. This simple proof can readily be extended for  $k$ -dependent  $V_\mu^{j,k,s}$ .

The physical reason that the doubly occupied and empty single-particle states give rise to a ferromagnetic contribution to  $J^{\mu\nu}$  is that in the intermediate state in second-order perturbation theory an electron (hole) that hops onto the island with spin parallel to that of the cluster has smaller energy than an electron (hole) with opposite spin orientation, due to the ferromagnetic exchange *on* the cluster. Therefore an electron (hole) on the substrate with spin parallel to that of the cluster can lower its kinetic energy more efficiently through hopping to the empty (doubly occupied) states. This is reflected by the smaller energy denominator in Eqs. (21) and (22).

Singly occupied levels, on the other hand, give an *antiferromagnetic* contribution to  $J^{\mu\nu}$ ,

$$J_s^{\mu\nu} = \frac{1}{S_0} \sum_{j=I+1}^A V_\mu^{j,k_f*} V_\nu^{j,k_i} \times \left( \frac{1}{\delta E_{+,\downarrow} - \epsilon_{I+1} + \epsilon_j} + \frac{1}{\delta E_{-,\downarrow} + \epsilon_A - \epsilon_j} \right), \quad (23)$$

with  $J_s^{\mu\nu}$  having only non-negative eigenvalues.<sup>22</sup> This is a result of the Pauli principle, because only electrons (holes) in states with spin antiparallel to that of the cluster may hop onto singly occupied levels in second-order perturbation theory, and thereby reduce their kinetic energy.

Equations. (21), (22), and (23) constitute one of the central results of the paper. They describe how  $J^{\mu\nu}$  depends on the density of states of the singly occupied levels on the cluster, the excitation energies to the  $N \pm 1$  manifold of states and the tunneling amplitudes to the various levels of the cluster.

In general, there is a competition among the three terms of Eq. (20), and thus the sign of eigenvalues of  $J^{\mu\nu}$  depends on the specific structure of the single-particle density of states on the cluster, and other mesoscopic parameters such as  $\delta E_{\pm, \sigma}$ . In the *absence* of ferromagnetic interactions on the cluster,  $U = 0$ , however, the ferromagnetic contributions  $J_e^{\mu\nu}$  and  $J_d^{\mu\nu}$  identically vanish, and the effective interaction is always antiferromagnetic, provided there is an odd number of electrons on the cluster.

The itinerant model has been used independently in Ref. 23 to describe spin  $S = 1$  metallic nanoclusters with similar results. In that case the ferromagnetic interaction is weak,  $U < \delta$ , the island is far from a ferromagnetic instability, and the  $S = 1$  ground state of the island results rather from two single-particle states of the island having energies accidentally closer than  $U < \delta$ . Then the ferromagnetic contribution of the doubly occupied and unoccupied levels is usually negligible, and the effective exchange interaction is dominated by the antiferromagnetic contributions of the singly occupied levels.<sup>23</sup>

The off-diagonal elements of  $J^{\mu\nu}$  are a sum of random numbers since the  $\varphi_j^*(\vec{R}_n) \psi_{\mu,k}(\vec{R}_n)$  of Eq. (18) have random phase for different  $j$  and  $\mu$ 's. Therefore the size of the off-diagonal elements of  $J^{\mu\nu}$  will be down by a factor of  $\sim \sqrt{1/2S_0} \sim \sqrt{\langle \delta_{A,I} \rangle / \Delta_s}$  compared to the diagonal ones with  $\mu = \nu$ , and the matrix  $J^{\mu\nu}$  will be dominated by the diagonal elements if the number of scattering channels  $M$  is much less than  $2S_0$ .

### B. Weak tunneling at a single point of contact

It is instructive and also useful to specialize the results of Sec. III A to the important case of a ferromagnetic cluster that makes contact with a metallic substrate in only a single point. Then we can choose a basis where  $J^{\mu\nu}$  consists of a single nonzero element as all but one conduction channel will decouple from the cluster (that is, a linear combination of the host orbital modes can be found such that only one orbital mode in the new basis has nonzero amplitude at the

impurity location). With the origin taken as a single point of contact,  $V_\mu^{j,k}$  of Eq. (18) reduces to  $V_j \equiv V\varphi_j^*(0)\psi_k(0)$ . Equation (23), e.g., then becomes

$$J_s = \sum_j \frac{|V_j|^2}{S_0} \left( \frac{1}{\delta E_{+,\downarrow} - \epsilon_{I+1} + \epsilon_j} + \frac{1}{\delta E_{-,\downarrow} + \epsilon_A - \epsilon_j} \right). \quad (24)$$

In the limit  $\Delta_s, \delta E_{\pm,\sigma} \gg \delta$  Eqs. (22), (21), and (23) can be approximately evaluated by assuming that the tunneling matrix amplitudes do not vary too much from level to level, and replacing the sums by integrals. For  $J_s$ , e.g., we obtain

$$J_s \approx \frac{\langle |V_j|^2 \rangle_j}{S_0} \int_0^{\Delta_s} d\xi \varrho(\epsilon_I + \xi) \left( \frac{1}{\delta E_{+,\downarrow} + \xi} + \frac{1}{\delta E_{-,\downarrow} + \Delta_s - \xi} \right), \quad (25)$$

with  $\varrho(\epsilon)$  the single-particle density of states on the cluster, and  $\langle |V_j|^2 \rangle_j$  the average hybridization strength. The ferromagnetic couplings  $J_d$  and  $J_e$  can be expressed by similar integrals. For  $S_0 \gg 1/2$  these integrals can be combined in a straightforward calculation where the integrand  $1/\delta E_{\pm,\sigma} + \xi$  is separated into the two regions  $\xi \gg \delta E_{\pm,\sigma}$  and  $\xi \ll \delta E_{\pm,\sigma}$  and then approximated in each region. We obtain the following estimate for the effective exchange coupling valid when  $\delta E_{\pm,\sigma} \gg \delta$ :

$$J^{\text{eff}} \sim \frac{\langle |V_j|^2 \rangle}{S_0} \left[ P \int_{-\infty}^{\infty} \frac{\Delta_s \varrho(\xi) d\xi}{(\xi - \epsilon_I)(\epsilon_A - \xi)} - \varrho(\epsilon_I) \ln \left( \frac{\delta E_{+,\downarrow}}{\delta E_{-,\uparrow}} \right) + \varrho(\epsilon_A) \ln \left( \frac{\delta E_{+,\uparrow}}{\delta E_{-,\downarrow}} \right) \right]. \quad (26)$$

This simple expression is one of the central results of this work. Equation (26) describes the dependence of  $J^{\text{eff}}$  on the *particular details of the density of states* of an itinerant ferromagnetic nanocluster. The first term involves a principal value integral (denoted by  $P$ ) over energy and clearly shows that whenever  $\epsilon_I < \xi < \epsilon_A$  the contribution to  $J^{\text{eff}}$  is antiferromagnetic; otherwise it is ferromagnetic, i.e., electron and hole excitations in the singly occupied states give rise to an antiferromagnetic coupling while electron (hole) excitations of the empty (doubly occupied) states give rise to a ferromagnetic contribution. The last two terms of Eq. (26) are *mesoscopic fluctuations* that depend on the specific charging energies of the nanocluster and the density of states at the top of the minority and majority bands. Other mesoscopic fluctuations come from variations in the tunneling matrix elements and in the level spacing, which are ignored in our model. These mesoscopic corrections become more pronounced for smaller cluster sizes and lead to strong fluctuations around  $J^{\text{eff}}$ .

For Co, the single-particle density of states has a maximum within the spin-polarized part of the spectrum,  $\epsilon_I < \xi < \epsilon_A$ , resulting in a  $J^{\text{eff}}$  that tends to be *antiferromagnetic*. Numerical evaluation of Eq. (26) using the actual density of states for cobalt<sup>20</sup> shows that the ferromagnetic contributions to  $J^{\text{eff}}$  from  $J_d$  and  $J_e$  reduce the dominant antiferromagnetic contribution from  $J_s$  by roughly 50–60%. Fluctuations of

$\delta E_{\pm,\sigma}$  in small clusters by a factor of 2 can lead to sample to sample fluctuations of  $\sim 10\%$  in  $J^{\text{eff}}$  for Co. This ultimately leads to large fluctuations in the Kondo temperature,  $T_K$ , from cluster to cluster, since  $J^{\text{eff}}$  appears in the exponent of the expression for  $T_K$ .

Equation (26) also describes how  $J^{\text{eff}}$  scales with cluster size. From the normalization of the cluster wave functions we find  $\langle |V_j|^2 \rangle \sim 1/N_A$ . Assuming that the magnetization of the cluster per atom is determined by microscopic mechanisms and thus  $U \sim \Delta_s$  does not depend on the cluster size, both  $S_0 \propto N_A$  and  $\varrho \propto N_A$ . This results in a fast decrease of  $J^{\text{eff}}$  with increasing cluster size (spin),  $J^{\text{eff}} \propto 1/N_A \propto 1/S_0$ , and therefore an exponentially suppressed  $T_K$ . Note that this suppression in  $T_K$  *depends only on the level structure* of the ferromagnetic nanocluster, not on any interference effects which may come from several points of contact.<sup>24</sup>

It is useful at this point to mention what would happen if  $U \ll \delta_{I,A}$  and we had an odd number of electrons on the cluster. There is then only one singly occupied level on the cluster, the sums in Eqs. (21) and (22) vanish, and the sum in Eq. (23) reduces to just two terms. As a result, for the spin 1/2 cluster,  $J_{1/2}^{\text{eff}} \propto \langle |V_j|^2 \rangle^2 / E_C \propto 1/N_A^{1-\alpha}$  with  $\alpha > 0$  since  $E_C \propto 1/N_A^\alpha$ . Thus, for sufficiently large  $N_A$ ,  $J^{\text{eff}}$  for the ferromagnetic cluster ( $U \gg \delta_{I,A}$ ) will scale to zero faster with  $N_A$  than for the nonmagnetic cluster. In Sec. IV B and in the conclusions, we will comment on what this means for the scaling of the Kondo temperature with the number of atoms in such a cluster.

### C. Weak tunneling at several points of contact

For tunneling at several points of contact we again turn to Eqs. (20–23). In this case,  $J^{\mu\nu}$  is necessarily a matrix reflecting the scattering of electrons in more than one orbital channel. As Eq. (18) shows, there will be significant random fluctuations in the matrix elements  $J^{\mu\nu}$  from the  $\varphi_j(\vec{R}_n)$  as cluster size is changed. For  $N_p$  points of contact there are a maximum of  $N_p$  orbital channels that will be scattered. However, if  $N_p$  is large, the number of orbital channels that are scattered may be much smaller. The largest angular momentum (orbital) channel scattered being  $l \sim L/\lambda_F$ , the matrix  $J^{\mu\nu}$  is approximately of size  $\sim l^2 \times l^2$  for a cluster in bulk or  $\sim l \times l$  for a cluster in contact with a two-dimensional electron gas. For a nanotube at most four orbital channels can scatter low-energy electrons.<sup>14</sup>

As we discussed earlier in this case, in principle at least, one may observe a series of Kondo effects. The cluster displays an underscreened Kondo effect, where the spin of the impurity is large and several channels with different coupling constants try to screen it. The channel with the largest coupling to the impurity screens half a spin first and ceases to interact with the impurity. Then the channel with the largest coupling from the remaining channels screens half a spin and so on. In practice, however, the various Kondo temperatures are exponentially separated, and the very small Kondo temperatures are likely to be much smaller than the spin-anisotropy energy of the cluster. Therefore in a realistic situation one can only observe one, or possibly two Kondo effects.<sup>25</sup>

#### IV. STM TUNNELING SPECTRA AND KONDO EFFECT

##### A. STM tunneling spectra of ferromagnetic clusters

In the simplest model of STM spectra the tip is treated as a point source of electrons and the resulting signal is proportional to the local density of states (LDOS) at the tunneling position  $\vec{r}$ ,<sup>26</sup>

$$\frac{dI}{dV}(\vec{r}, V) \propto \text{LDOS}(\vec{r}, \omega = eV) \equiv -\frac{1}{\pi} \text{Im}[G^R(\vec{r}, \omega = eV)]. \quad (27)$$

Here  $G^R(\vec{r}, \omega)$  is the retarded Green's function of the substrate below the tip, and  $V$  is the voltage difference between the STM tip and the substrate. Below we consider only tunneling directly into the cluster, ignoring any Fano-type interference effects.<sup>9,10</sup>

Let us first focus on the high-energy part of the spectrum at  $\omega > T_K$ , where the Kondo-type strong correlations are negligible. Using standard manipulations we can express the retarded Green's function as

$$\begin{aligned} G^R(\vec{r}, \omega) \approx & \frac{1}{N_G} \sum_{G, E, E'} \left[ \langle G | \hat{\phi}(\vec{r}) | E \rangle \right. \\ & \times \left( \frac{1}{[\omega - (\hat{E} - E_G)] - M^R(\omega)} \right)_{EE'} \langle E' | \hat{\phi}^\dagger(\vec{r}) | G \rangle \\ & + \langle G | \hat{\phi}^\dagger(\vec{r}) | E \rangle \left( \frac{1}{[\omega + (\hat{E} - E_G)] - M^R(\omega)} \right)_{EE'} \\ & \left. \times \langle E' | \hat{\phi}(\vec{r}) | G \rangle \right], \quad (28) \end{aligned}$$

where now  $|E\rangle$  denotes excited states of the system in the *absence* of tunneling, i.e.,  $|E\rangle$  is a direct product of the excited states of the isolated cluster and the excited states of the isolated substrate and  $\hat{E} = \delta_{E, E'}$ . The operator  $\hat{\phi}^\dagger(\vec{r})$  ( $\hat{\phi}(\vec{r})$ ) creates (annihilates) an electron at position  $\vec{r}$  on the cluster. We average over the ground-state multiplet  $|G\rangle$  with degeneracy  $N_G = 2S_0 + 1$ , and  $M^R$  is the generalized retarded self-energy matrix.

Assuming that  $\Gamma_0^j \equiv 2\pi \varrho_0 \sum_\mu |V_\mu^j|^2 < \min\{\delta E_{\pm, \sigma}^j, \delta_A, \delta_I\}$ , we can do perturbation theory in the tunneling. In this case the ground state  $|G\rangle$  can be approximated in leading order by the product of the independent ground states of the cluster and the metal, and the summation over the excited states  $|E\rangle$  turns into a sum over the states  $|E_{\pm, \sigma}^j\rangle$  defined in Sec. II (see Fig. 2). With these assumptions the retarded self-energy  $M^R(\omega)$  is approximately diagonal in  $E$  and  $E'$ ,

$$M^R(\omega)_{EE'} \approx (\text{real part}) - i \delta_{EE'} \pi \sum_n \delta(\omega - E_n) |\langle n | \hat{V} | E \rangle|^2, \quad (29)$$

where summation is carried out over all possible intermediate states  $|n\rangle$  and  $\hat{V}$  is given by Eq. (17). The real part of the

self-energy produces only a slight shift of the levels, and it can be neglected. The imaginary part, on the other hand, describes the broadening of the spectrum.

Within these approximations the STM spectrum can be expressed as

$$\frac{dI}{dV} \propto \sum_{j, \sigma, \pm} |\varphi_j(\vec{r})|^2 \frac{\Gamma_{\pm, \sigma}^j}{(\omega \mp \delta E_{\pm, \sigma}^j)^2 + (\Gamma_{\pm, \sigma}^j/2)^2} \quad (30)$$

where  $\Gamma_{\pm, \sigma}^j$  is the total decay rate of the excited state with excitation energy  $\delta E_{\pm, \sigma}^j$ .

Equation (30) assumes that no two states of the cluster in the same spin sector are closer to each other than  $\Gamma_0$ . Otherwise they may produce Fano-type resonances due to the interference between electrons (or holes) that tunnel through these states. For our mean field models with maximum level repulsion, however, this condition is always satisfied if  $\Gamma_0 < \delta_I, \delta_A$ . Also, if the ground-state energy difference for the cluster with  $N$  and  $N \pm 1$  electrons on it (or with spin  $S_0$  and  $S_0 \pm 1$ ) is too small compared to  $\Gamma_0$  the initial state will not have a definite electron number (or spin) and our computation breaks down.

For  $\delta E_{\pm, \sigma}^j > \delta_{A, I}$  we find that the decay rate  $\Gamma_{\pm, \sigma}^j$  is typically larger than the single-particle tunneling rate  $\sim \Gamma_0^j$ . This can be understood as follows. Assuming that the STM-cluster voltage is already large enough to overcome the Coulomb blockade, an energy  $\sim E_C/2$  is transferred to the cluster as an electron or hole hops onto the cluster from the STM tip. The extra charge carrier then tunnels into the leads. However, for  $\delta E_{\pm, \sigma}^j > \delta_{A, I}$  the island can be left behind in a state that contains electron-hole excitations. Assuming for the sake of simplicity that  $\Gamma_0^j = \Gamma_0$  is independent of the single-particle state index  $j$ , we obtain the result that the width of a given level is proportional to the number of ways it can decay:  $\Gamma_{\pm, \sigma}^j \approx N_{\text{decay}}^{(j, \pm, \sigma)} \Gamma_0$ , where  $N_{\text{decay}}^{(j, \pm, \sigma)}$  is the number of island states with  $N$  electrons whose energy  $E(N) - E_G < \delta E_{\pm, \sigma}^j$  and which are accessible by the addition (or subtraction) of just one electron from the state corresponding to  $\delta E_{\pm, \sigma}^j$ . There is no simple expression for the  $N_{\text{decay}}^{(j, \pm, \sigma)}$ 's; they depend sensitively on the level  $j$ ,  $N_A$ ,  $E_C$ , and the *fluctuating* mesoscopic parameters  $d_0$  and  $n_g$ , and we have to determine them for each set of parameters and each level separately.

Within the mean-field model we are using and to leading order in the tunneling  $\hat{V}$  the number of decay channels of the state with energy  $E_{\pm, \sigma}^j$  does not depend on  $j$ . This is an artifact of the mean-field approximation. In higher orders of the tunneling (virtual tunneling processes) or in the presence of electron-electron interactions on the island (which may also change level occupations) excited states with larger energies generally have a larger decay amplitude. Examples of decay processes for a given excited state are shown in Fig. 4.

According to Eq. (30), the weakly coupled cluster spectrum is simply a series of Lorentzian peaks centered at the particle and hole addition energies determined by Eq. (1), Eq. (5), and the actual band structure of Co (Ref. 20) with a weight modulated by a random amplitude  $|\varphi_j(\vec{r})|^2$ . In our

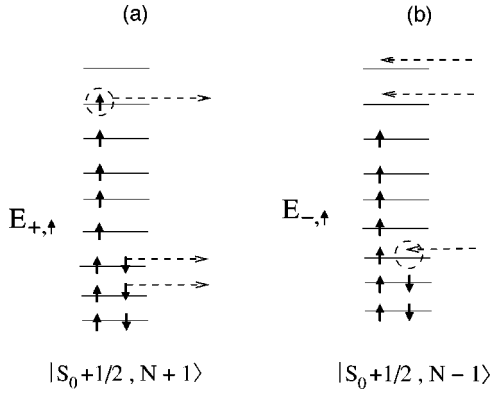


FIG. 4. The dashed lines represent possible decay channels for the states  $|E_{+,↑}\rangle$  ( $N+1$  electrons) and  $|E_{-,↑}\rangle$  ( $N-1$  electrons) to lower energy states with  $N$  electrons. In an actual decay, only one of the processes indicated by the dashed lines would occur.

calculation (See Fig. 5) of the STM tunneling conductance we ignore (i) the amplitude modulation, (ii) fluctuations in the level spacing of the cluster beyond that given by band-structure calculations<sup>20</sup> (as we discussed in Sec. II), and (iii) fluctuations in the hybridization  $\Gamma_0^j \approx \Gamma_0$ . These effects could be included with some effort, but they would not be expected to change our conclusions.

In principle, contributions from phonon scattering or electron-electron interactions also contribute to the relaxation rate  $\Gamma_{\pm,\sigma}^j$ ; however, in the experiments of Ref. 7 these

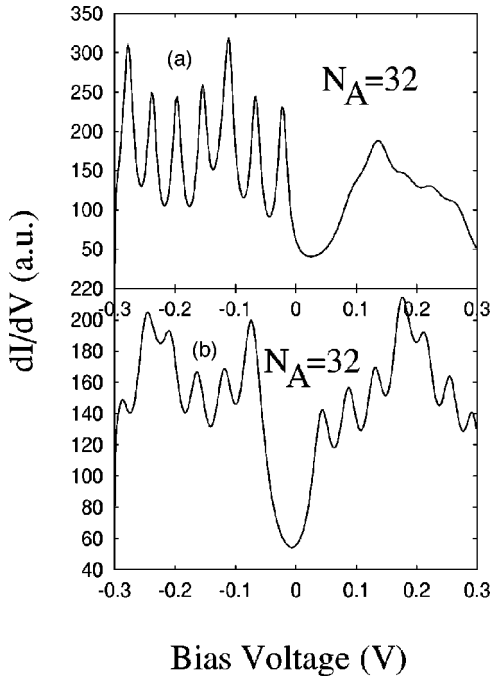


FIG. 5. Calculated STM spectra of nanometer-size ferromagnetic clusters with parameters  $N_A=32$ ,  $E_C^+=0.01$  eV,  $E_C^-=0.08$  eV,  $\Gamma_0=0.02$  eV, and  $\mu=0$  at 4 K (see main text). We took  $\Gamma_0^j=2\pi|V_j|^2\rho_0\approx\Gamma_0$ , independent of  $j$ , and  $|\varphi(\vec{r})|^2=\text{const}$  in Eq. (30). In (a) we set  $d_0=0.07$  eV while in (b)  $d_0=-0.05$  eV. The difference between the two cases demonstrates the sensitivity to mesoscopic parameters.

can probably be neglected with respect to the single-particle relaxation channel considered here.

To compute the tunneling spectrum of an actual cluster with  $N_A$  atoms we generated a discrete set of levels  $\epsilon_j$  with a level spacing corresponding to the single-particle density of states in Co.<sup>20</sup> As discussed above, the nonuniform density of states is important to obtain a predominantly antiferromagnetic coupling, but is also important to obtain a stable ground state with a partially polarized band. The STM spectrum for low bias voltages is governed by the level structure near  $\epsilon_A$  and  $\epsilon_I$  since these are the only states probed in an STM measurement at low voltage bias. The majority and minority level spacing at these energies can be estimated from band-structure calculations as  $\delta_A=5.55$  eV/ $N_A$ ,  $\delta_I=1.43$  eV/ $N_A$  and  $S_0=0.855N_A$ .<sup>20</sup> For Co,  $\Delta_s=\epsilon_A-\epsilon_I\approx 2$  eV.

For the sake of simplicity we set  $\bar{\epsilon}=(\epsilon_I+\epsilon_A)/2=0$  in our computations, effectively absorbing it into  $n_g$ . This corresponds to a specific choice of contact potential between the lead and the cluster, and does not influence the overall features of the spectrum.

Equation (30) assumes the cluster is in its ground state before the electron from the STM tunnels into it. Thus, in the numerical calculation it is important to ensure that the parameters of the model give a ground state with definite  $S_0$  and  $N$ . Using Eq. (1) and Eq. (5) and keeping track of the  $1/N_A$  corrections which are all put into  $d_0$ , one can derive the conditions for stability of the ground state, which we assume to have  $N_s\approx 1.71N_A$  singly occupied levels. By considering the fluctuations in the ground-state spin shown in Figs. 1(b) and 1(c) one can show that to guarantee stability,  $d_0$  must satisfy the conditions

$$-\frac{N_A}{S_0}\delta_I < d_0 < \frac{N_A}{(S_0+1)}\left(\delta_A - \frac{\Delta_s}{S_0}\right). \quad (31)$$

For Co this simplifies to  $-1.67$  eV/ $N_A < d_0 < 3.21$  eV/ $(0.855N_A+1)$ . Similar conditions can easily be derived for the quantities  $E_C^+$  and  $E_C^-$  by considering fluctuations to the  $N\pm 1$  manifold of states like those in Fig. 2 and requiring  $\delta E_{\pm,\sigma} > 0$ . For our model applied to Co we obtain  $E_C^+ > -1.0$  eV/ $N_A$  and  $E_C^- > 2.48$  eV/ $N_A$ .

A calculation of the tunneling spectrum of a ferromagnetic cluster with  $N_A=32$  atoms and a corresponding spin  $S_0=27$  is shown in Fig. 5. For the computations we used the parameters  $E_C^+=0.01$  eV,  $E_C^-=0.08$  eV and  $\Gamma_0=0.02$  eV in both figures. Then once  $d_0$  is given all the  $\delta E_{\pm,\sigma}^j$  are determined via relations similar to Eq. (8). The quantity  $N_{\text{decay}}^{(j,\pm,\sigma)}$  is computed numerically. In Fig. 5(a)  $d_0=0.07$  eV, and the ground state is close to being unstable against the lowest lying state within the  $(N, S_0+1)$  subspace, while in Fig. 5(b)  $d_0=-0.05$  eV, and the ground state is close to the lowest lying state within the  $(N, S_0-1)$  subspace.

In the spectrum in Fig. 5(a) there is a series of sharp peaks at negative bias (electrons are removed from the cluster) while the spectrum at positive bias (electrons are added to the cluster) is rather smooth. These features correspond very well with asymmetrical features seen in some spectra of Ref. 7. On the other hand, the lower spectra of Fig. 5(b) have less

contrast between positive and negative biases. The only parameter that has been changed between the two spectra is  $d_0$  of Eq. (5). Different values of  $d_0$  lead to different values of the number of decay channels  $N_{\text{decay}}^{(j,\pm,\sigma)}$  for positive and negative bias, and hence lead to different widths of the peaks in  $dI/dV$ . This calculation shows how mesoscopic fluctuations may make a significant qualitative difference in the spectra of two clusters with the same  $N_A$ ,  $E_C$ , and  $n_g$ . For real clusters mesoscopic fluctuations in  $E_C$  and  $n_g$  are also expected for fixed  $N_A$  and these will also lead to qualitative changes in the spectra.

A careful comparison of our calculated spectra corresponding to the first few charging peaks with the experimental spectra shows that at voltage biases up to  $\approx \pm E_C$  our calculations are in agreement with experiment, however, at larger biases,  $eV > E_C$  [when *two* additional electrons (or holes) could be added to the cluster at the same time], the experimental spectra show additional structure, not present in our calculations, presumably due to many body and/or nonequilibrium excitations left out of our simple model.

As we will see in the following section, for the cluster size of Fig. 5 the estimated Kondo temperature is significantly below the experimental temperature, and no Kondo peak appears at zero bias.

## B. Estimating the Kondo temperature

It is obvious that Eq. (30) does not include Kondo correlations and therefore does not produce a Kondo peak in the spectrum. However, it is generally true that when the Kondo effect is present, it produces a peak of width  $\sim T_K$  at the Fermi level with relative weight  $\sim T_K/\Gamma_0$  due to the approximate unitary scattering, provided the temperature is less than  $T_K$ ,  $T < T_K$ .<sup>1,15</sup>

In order to estimate  $T_K$  and its dependence on cluster size, we will use the results of Sec. III B for a cluster contacting the substrate in only a single point of contact. There are several reasons why we believe this may be a reasonable assumption to make for Co nanoclusters on metallic nanotubes.<sup>7</sup> First of all, the ratio of broadening  $\Gamma$  of energy levels on the cluster compared to their separation  $\sim \delta_{A,I}$  is experimentally found to be almost independent of the cluster size. Since  $\delta_{A,I} \sim 1/N_A$  and  $\Gamma \sim N_P/N_A$  ( $N_P$  is the number of points of contact), this indicates that the number of effective tunneling points is approximately constant for the clusters investigated in the measurements.<sup>27</sup> In fact, since the diameter of the clusters (0.5–1 nm) of Odom *et al.*<sup>7</sup> are comparable to the diameter of a nanotube there is appreciable curvature at the cluster-nanotube interface, and it is quite possible that the cluster touches the surface of the nanotube only at a few points. Since the tunneling amplitude is exponentially sensitive to the tunneling distance, it is also possible that only one or two of these points dominates the conductance between the cluster and the nanotube, resulting effectively in a coupling in the form of a single point of contact.

The standard expression for the Kondo temperature in the Kondo model is given by<sup>1</sup>

$$T_K = D \sqrt{J^{\text{eff}} \varrho_0} e^{-1/J^{\text{eff}} \varrho_0}, \quad (32)$$

where  $D$  is the bandwidth of the conduction electrons of the metallic host and  $\varrho_0$  is the density of states of the host at the impurity site. For a ferromagnetic cluster, however, this formula is incorrect, since the Kondo Hamiltonian provides an appropriate description of the cluster dynamics only below the characteristic energy of inelastic excitations,  $E_{\text{inel}} \equiv \min\{E_C, \delta_{A,I}\}$ . As shown, for example, in the two-level system model,<sup>28</sup> above this energy scale fluctuations to various excited states destroy the coherent spin processes leading to the Kondo effect, and in the renormalization-group approach in the regime above  $E_{\text{inel}}$  the Kondo coupling remains unrenormalized. Therefore, for a single point of contact we estimate the Kondo temperature as

$$T_K \sim \min\{E_C, \delta_{A,I}\} \sqrt{J^{\text{eff}} \varrho_0} e^{-1/J^{\text{eff}} \varrho_0}, \quad (33)$$

where we replaced the bandwidth  $D$  of the conduction electrons by the energy gap for inelastic processes on the cluster,  $D \rightarrow \min\{E_C, \delta_{A,I}\}$ . Equation (33) is only of logarithmic accuracy. In general,  $T_K$  contains an overall prefactor that incorporates corrections from higher excited states as well as possible mesoscopic fluctuation effects. This prefactor is usually of the order of unity, however, in some cases it can be quite large and considerably increase the Kondo temperature.<sup>29</sup>

In principle, the quantities  $E_C$  and  $\delta_{A,I}$  can be obtained directly from the STM spectra, and  $J^{\text{eff}} \varrho_0$  can also be related to the spectra via the width of the energy levels of the cluster. Recalling  $\Gamma_0^j = 2\pi |V_j|^2 \varrho_0$  we can write

$$J^{\text{eff}} \varrho_0 \approx \frac{\Gamma_0}{2\pi S_0} \left[ P \int_{-\infty}^{\infty} \frac{\Delta_s \varrho(\xi) d\xi}{(\xi - \epsilon_I)(\epsilon_A - \xi)} - \varrho(\epsilon_I) \ln \left( \frac{\delta E_{+, \downarrow}}{\delta E_{-, \uparrow}} \right) + \varrho(\epsilon_A) \ln \left( \frac{\delta E_{+, \uparrow}}{\delta E_{-, \downarrow}} \right) \right], \quad (34)$$

where we have used Eq. (26) and taken  $|V_j|^2 \rightarrow \langle |V_j|^2 \rangle$ . Recall that  $\varrho(\epsilon) \propto N_A$ .

As is evident from Eq. (30), the actual level width of cluster excited states observed in experiment is  $\Gamma^j = N_{\text{decay}} \Gamma_0^j$ , where  $N_{\text{decay}}$  is the number of energetically allowed decays for a particular excited state in the  $N \pm 1$  manifold as described in Sec. IV A. According to our model STM spectra calculations (Sec. IV A) (which computes  $N_{\text{decay}}^{(j,\pm,\sigma)}$  numerically)  $N_{\text{decay}}$  is typically 1–3 for clusters with 7–30 atoms. As the most favorable case for obtaining an experimentally consistent  $T_K$ , we take  $N_{\text{decay}} = 1$  in our estimates.

To obtain an estimate of the Kondo temperature for Co atoms adsorbed on nanotubes we used the experimental data of Ref. 7. For a cluster experimentally estimated to have  $N_A = 8$  atoms, the value  $\Gamma \sim 0.24$  eV and  $E_C \sim 0.36$  eV can be directly determined from the experimental STM spectrum of cluster. Unfortunately, the level spacing  $\delta_{I,A}$  cannot be determined directly from the STM spectra for these small clusters, but can we estimate them by rescaling the level spacing measured at larger clusters, giving  $\delta_I \sim 0.24$  eV.

Assuming that the spin splitting takes its bulk value,  $\Delta_s \sim 2$  eV we can then estimate  $T_K$  using Eqs. (34) and (33).

We numerically evaluated both the integral in Eq. (26) as well as the discrete sums in Eqs. (21)–(23) using the actual Co density of states<sup>20</sup> (assuming a single point of electrical contact). Neglecting the mesoscopic fluctuations in  $\delta E_{\pm,\sigma}$ , the integral and the discrete sum were found to be within 10% of each other for  $N_A = 8, 16,$  and  $32$ . The Kondo temperature estimated this way for  $N_A = 8$ ,  $T_K \sim 0.16$  K turned out to be about a factor 500 smaller than the experimentally observed Kondo temperature,  $T_K^{\text{exp}} \sim 80$  K. (We obtain a value of  $J^{\text{eff}} \varrho_0 = 0.12$  for  $N_A = 8$ . This would need to be increased by a factor of  $\sim 2.5$  to reach agreement with experiment.) Mesoscopic fluctuations of  $E_{\pm,\sigma}$  may increase (or decrease)  $J^{\text{eff}}$  by  $\sim 10\%$ . Furthermore, our integrals (and sums) were evaluated with the assumption that  $V_j$  is independent of energy. This is not strictly true and will lead to additional fluctuations in  $J^{\text{eff}}$ . These mesoscopic fluctuation effects typically change the value of  $J^{\text{eff}}$  altogether by 10–15%. It seems unlikely that such fluctuations could bring the theoretical estimate of  $T_K$  into the experimentally observed range. Thus, there is a discrepancy between experiment and theory. There may be several explanations for this disagreement that we discuss in detail in Sec. VI of the paper.

Equation (34), on the other hand, is in qualitative agreement with the experiments in that it predicts an extremely rapid decrease of  $T_K$  with increasing cluster size. Since for a single point of contact  $\Gamma_0 \sim 1/N_A$ ,  $S_0 \sim N_A$ , and  $\varrho(\xi) \sim N_A$ , the dimensionless exchange coupling scales as  $J^{\text{eff}} \varrho_0 \sim 1/N_A$ . We also verified numerically that the scaling  $J^{\text{eff}} \propto 1/N_A$  of Eq. (26) is maintained for the discrete sum in Eqs. (21)–(23).

Note that if one were to assume multiple contacts between the cluster and substrate, while keeping the decay rate fixed, then one would obtain smaller values for the typical tunneling matrix element  $V_{\mu}^{j,k}$  and, hence, a lower Kondo temperature.

As we found in Sec. III B, the dimensionless coupling constant for a nonmagnetic cluster,  $J_{1/2}^{\text{eff}} \varrho_0 \sim 1/N_A^{1-\alpha}$ , so that

the Kondo temperature is suppressed less rapidly with increasing  $N_A$ . In this sense, the large spin of a ferromagnetic cluster does not “help” the Kondo effect in any way.

## V. LOCAL MOMENT CLUSTERS

### A. Local moment mean-field model

In many magnetic materials it is more appropriate to think of a localized  $d$  or  $f$  level (as in the Anderson model) than to think of strongly hybridized  $s$ ,  $p$ , and  $d$  bands. These local moments may couple to each other ferromagnetically and produce ferromagnetism.

For small enough magnetic clusters with large enough Curie temperature, at low enough temperature the local moments form a large and rigid ferromagnetic spin,  $S_d$ , that couples to the extended states (a “conduction band”) of  $s$  and  $p$  character. The simplest Hamiltonian that one can conceive to describe this situation reads

$$\hat{H}_{\text{cluster}} = \sum_{j,\sigma} \epsilon_j c_{j\sigma}^\dagger c_{j\sigma} + \frac{J}{N_A} \hat{S}_c \cdot \hat{S}_d + \frac{E_C}{2} (\hat{N} - n_g)^2, \quad (35)$$

with  $\hat{S}_c$  and  $\hat{S}_d$  the total spin of the extended states and the local moments, respectively. A justification of Eq. (35) is given in Appendix A. Similar to the itinerant model, the first term describes the kinetic energy of the extended electron states, and the third term accounts for the finite charging energy of the cluster. The second term of Eq. (35) describes the exchange interaction between the local moments and the extended states and tends to polarize the latter. We assume in what follows that the total spin of the conduction electrons is much smaller than that of the localized electrons. The exchange  $J$  is typically antiferromagnetic,  $J > 0$ , and the conduction electrons are polarized opposite to  $d$  electrons.<sup>30</sup>

The local moment model has  $S_T, S_T^z$  (the total spin and its  $z$  component),  $\{n_j\}$ ,  $S_d$ , and  $S_c$  as conserved quantum numbers, and can thus be diagonalized exactly. The ground state is given by

$$|S_T, S_T^z\rangle_{S_c, S_d}^N = \sum_{S_c^z, S_d^z; S_c^z + S_d^z = S_T^z} \langle S_c, S_d; S_c^z, S_d^z | S_T, S_T^z \rangle |S_c, S_d; S_c^z, S_d^z\rangle^N, \quad (36)$$

where  $|S_c, S_d; S_c^z, S_d^z\rangle^N = |S_d, S_d^z\rangle |S_c, S_c^z\rangle^N$  and  $S_T = S_d - S_c$  if  $J > 0$ . The state  $|S_c, S_c\rangle^N$  can be computed from Eq. (3) with  $S_c$  replacing  $S_0$  everywhere, and  $|S_c, S_c^z\rangle^N$  is computed from Eq. (4) with  $S_c$  replacing  $S_0$  and  $S_c^z$  replacing  $S^z$ .

Stability of the ground state implies the relation

$$J = \frac{N_A}{(S_d + 1)} \Delta_s + O(1/N_A), \quad (37)$$

where  $\Delta_s$  is now the band splitting of the conduction band.

Considering the type of particle-hole excitations shown in Fig. 1 and using Eq. (37), one finds that the excitation spectrum is very similar to that of the itinerant model. In particu-

lar, we find that for charge fluctuations  $\delta E_{\pm,\sigma} \sim E_C/2$ , and spin fluctuations have a gap  $\sim \delta_A, \delta_I$ .

### B. Computation of the exchange coupling

The coupling constants  $\tilde{J}^{\mu\nu}$  of the local moment model depend on the sign of the exchange coupling,  $J$ , of Eq. (35). Let us first focus on the case  $J > 0$  and  $S_d > S_c$ . For the local moment model,  $\langle f | \hat{H}_{\text{Kondo}}^{\text{eff}} | i \rangle = 1/2 \sqrt{2} S_T \tilde{J}^{\mu\nu}$ . To evaluate the RHS of Eq. (19) we must again evaluate contributions from the conduction electron states with double, single, and no occupation,

$$\tilde{J}^{\mu\nu} = \tilde{J}_d^{\mu\nu} + \tilde{J}_s^{\mu\nu} + \tilde{J}_e^{\mu\nu}. \quad (38)$$

For the sake of simplicity, let us consider the contribution of singly occupied levels,  $\tilde{J}_s^{\mu\nu}$ . Various matrix elements of the type  $_j^{N+1}\langle S_T+1/2, S_T-1/2 | c_{j\downarrow}^\dagger | S_T, S_T \rangle^N$  arise in course of the evaluation of  $\tilde{J}^{\mu\nu}$ , and in contrast to the itinerant cluster model, the intermediate states of the local moment model (with  $J>0$  and  $S_d>S_c$ ) have an *increase* in total spin on the cluster in this case. To evaluate  $_j^{N+1}\langle S_T+1/2, S_T-1/2 | c_{j\downarrow}^\dagger | S_T, S_T \rangle^N$  we first expand  $|S_T, S_T\rangle_{S_c, S_d}^N$  and  $|S_T+1/2, S_T-1/2\rangle_{S_c-1/2, S_d}^{N+1}$  using Eq. (36) to obtain

$$\begin{aligned} &_j^{N+1}\langle S_T+1/2, S_T-1/2 | c_{j\downarrow}^\dagger | S_T, S_T \rangle^N \\ &= \sum_{S_c^z = -S_c}^{S_c} \langle S_c, S_d; S_c^z, S_T - S_c^z | S_T, S_T \rangle \\ &\quad \times \langle S_c - 1/2, S_d; S_c^z - 1/2, S_T - S_c^z | S_T + 1/2, S_T - 1/2 \rangle_j^{N+1} \\ &\quad \times \langle S_c - 1/2, S_c^z - 1/2 | c_{j\downarrow}^\dagger | S_c, S_c^z \rangle^N. \end{aligned} \quad (39)$$

What remains to be computed in Eq. (39) is the matrix element  $_j^{N+1}\langle S_c - 1/2, S_c^z - 1/2 | c_{j\downarrow}^\dagger | S_c, S_c^z \rangle^N$ . To determine this, we use the states of Eq. (4) with  $S_c$  replacing  $S_0$ . The overlap is computed by first directly evaluating  $_j^{N+1}\langle S_c - 1/2, S_c - 1/2 | c_{j\downarrow}^\dagger | S_c, S_c \rangle^N$  and then applying the Wigner-Eckhart Theorem for general  $S_c^z$ . This yields  $_j^{N+1}\langle S_c - 1/2, S_c^z - 1/2 | c_{j\downarrow}^\dagger | S_c, S_c^z \rangle^N = \sqrt{S_c + S_c^z/2} S_c$ . This can then be substituted into Eq. (39) which finally gives

$$\begin{aligned} &_j^{N+1}\langle S_T+1/2, S_T-1/2 | c_{j\downarrow}^\dagger | S_T, S_T \rangle^N \\ &= \sum_{S_c^z = -S_c}^{S_c} \sqrt{\frac{S_c + S_c^z}{2S_c}} \langle S_c, S_d; S_c^z, S_T - S_c^z | S_T, S_T \rangle \\ &\quad \times \langle S_c - 1/2, S_d; S_c^z - 1/2, S_T - S_c^z | S_T + 1/2, S_T - 1/2 \rangle \end{aligned} \quad (40)$$

The results of the evaluation of all the matrix elements on the right-hand side of Eq. (19) for the local moment model as well as the expression equivalent to Eq. (20) are somewhat lengthy, so we relegated them to Appendix B. We evaluated them numerically for  $S_T = S_d - S_c$  (antiferromagnetic  $J$  and  $S_d > S_c$ ) and found that the single-particle contribution to the final exchange coupling differs in an overall sign from the itinerant model result of Sec. III, and it is ferromagnetic. On the other hand, if  $J$  is ferromagnetic, then  $S_T = S_d + S_c$  and the matrix elements above agree in sign with those of Sec. III.

This can qualitatively be understood as follows. Suppose the total spin,  $S_T$ , of the cluster points upward. Then by assumption  $S_d > S_c$  the spin of the  $d$  levels,  $S_d$ , also points up. If the internal interaction,  $J$ , between  $S_d$  and  $S_c$  is antiferromagnetic, delocalized electrons of the cluster with spin down will partially screen the local spin,  $S_d$ , so that the singly occupied states tend to have spin down. A substrate conduction electron that hops on a singly occupied state must have, therefore, spin up that is parallel to the total

spin, resulting in a ferromagnetic contribution to the effective interaction between the total cluster spin and the substrate. On the other hand, due to the antiferromagnetic interaction with the local spin, hopping to empty states with spin down have an energy smaller than those with spin up (parallel to the total spin), and give rise to an antiferromagnetic contribution to the effective interaction between the cluster spin and the substrate. The case  $J < 0$  can be understood along the same lines.

Similar to the itinerant case, the signs of  $\tilde{J}_d^{\mu\nu}$ , and  $\tilde{J}_e^{\mu\nu}$  are always opposite to that of  $\tilde{J}_s^{\mu\nu}$  regardless of the sign of  $J$ . Therefore, there is in general a competition between these terms, and the sign of the final coupling depends on specific band-structure features.

For an antiferromagnetic coupling,  $J > 0$ , in the limit where  $\Delta_s, E_C \gg \delta$ , and  $S_c, S_d, S_T \gg 1$  we can obtain the following simple estimate for a single point of contact, analogous to Eq. (34):

$$\begin{aligned} \tilde{J}^{\text{eff}} \varrho_0 \sim & -\frac{\langle |V_j|^2 \rangle}{S_T} \left[ P \int_{-\infty}^{\infty} \frac{\Delta_s \varrho(\xi) d\xi}{(\xi - \epsilon_l)(\epsilon_A - \xi)} \right. \\ & \left. - \varrho(\epsilon_l) \ln \left( \frac{\delta E_{+, \uparrow}}{\delta E_{-, \downarrow}} \right) + \varrho(\epsilon_A) \ln \left( \frac{\delta E_{+, \downarrow}}{\delta E_{-, \uparrow}} \right) \right]. \end{aligned} \quad (41)$$

The sign of the effective coupling depends on the sign of  $S_c - S_d$  (here given for  $S_c - S_d < 0$ ). For completeness, we also give the expression for  $J < 0$ , which does not depend on the relative size of  $S_c$  and  $S_d$  (note changes in mesoscopic fluctuations and overall sign),

$$\begin{aligned} \tilde{J}^{\text{eff}} \varrho_0 \sim & \frac{\langle |V_j|^2 \rangle}{S_T} \left[ P \int_{-\infty}^{\infty} \frac{\Delta_s \varrho(\xi) d\xi}{(\xi - \epsilon_l)(\epsilon_A - \xi)} \right. \\ & \left. - \varrho(\epsilon_l) \ln \left( \frac{\delta E_{+, \downarrow}}{\delta E_{-, \uparrow}} \right) + \varrho(\epsilon_A) \ln \left( \frac{\delta E_{+, \uparrow}}{\delta E_{-, \downarrow}} \right) \right]. \end{aligned} \quad (42)$$

These expressions are particularly interesting. However large the constituent spins ( $S_c, S_d$ ) of the cluster are, the cluster may still have a large effective coupling  $\tilde{J}^{\text{eff}}$  if the coupling  $J$  between  $S_d$  and  $S_c$  is antiferromagnetic ( $J > 0$ ) and the total spin is sufficiently small. In most cases  $S_c < S_d$ , therefore  $\tilde{J}^{\text{eff}}$  is ferromagnetic and no Kondo effect develops. For  $S_c > S_d$ , however,  $\tilde{J}^{\text{eff}}$  changes sign (still assuming  $J > 0$ ) and becomes antiferromagnetic. In this case a Kondo effect occurs with an effective coupling proportional to  $\sim 1/S_T$ .

It should be pointed out that the results described above are valid only in the weak tunneling limit. In the strong tunneling limit, the relative signs of  $\tilde{J}^{\text{eff}}$  and  $J$  are switched. For example, when the ‘‘internal’’ interaction  $J > 0$  and the cluster is in the *strong* tunneling regime one cannot distinguish the cluster wave functions from those of the host. Thus, the  $\tilde{J}^{\text{eff}}$  would have the same sign as  $J$ . Therefore we expect in this case  $J_{\text{eff}}$  to change sign as one gradually increases the tunneling between the cluster and the substrate. We have not studied in detail how this transition would occur.

## VI. DISCUSSION

This work grew out of an effort to better understand the experiments of Odom *et al.*<sup>7</sup> in which Kondo effect was observed at low temperatures  $\sim 5$  K for subnanometer Co particles adsorbed on metallic carbon nanotubes. Our model correctly predicts a Kondo temperature that decreases quickly with increasing cluster size, however, our numerical estimates of  $T_K$  tend to be too small by a factor of  $\sim 500$  for a cluster with  $N_A=8$ .

There may be several explanations for our low estimate of  $T_K$ .

(a) Mesoscopic fluctuations in Eq. (26) can eventually increase the effective Kondo coupling and thus bring  $T_K$  close to its experimental value. However, since the sign of the mesoscopic fluctuations is random, this interpretation would appear to contradict the experiments in which a significant fraction of small Co clusters produced a Kondo effect.

In addition to fluctuations in the various charging energies, the tunneling parameters  $V_j$  and the level positions  $\epsilon_j$  also fluctuate from cluster to cluster. These additional fluctuations were neglected in Eq. (26), since their contributions decrease with increasing cluster size. For small clusters, however, they may produce important additional fluctuations in  $J^{\text{eff}}$ .

(b) It appears furthermore that the experiments were performed close to the mixed valence regime as the width of the levels is comparable to the Coulomb charging gap. The effective Kondo Hamiltonian we derived in second-order perturbation theory may not adequately predict  $T_K$  in that case. In general, approaching the mixed valence regime the Kondo temperature becomes larger than expected by the naive Kondo model calculation, the Coulomb gap shrinks, and the Kondo resonance gradually merges with the high-energy part of the spectrum.

(c) It could be possible that some of the Co atoms in the cluster are not strongly attached to the others, and in the STM spectrum one observes the signal of these individual atoms. This explanation is, however, very unlikely in our opinion, because the Co atoms show a very strong tendency to cluster formation, and moreover the Kondo resonance is observed rather uniformly over the surface of clusters which are supported on nanotubes.

(d) In our analysis, we assumed that the anisotropy energy is smaller than the Kondo temperature, and therefore neglected it. However, it is conceivable that very small clusters have a considerably larger anisotropy than our estimates based on experiments on large clusters.<sup>17</sup> According to the STM measurements,<sup>7</sup> Co clusters in the nanotube experiments tend to have a ‘‘pancake shape’’ and the relative position of the Co atoms is probably strongly modified with respect to the bulk due to the presence of the substrate. Although the value of spin-orbit interaction on cobalt is not particularly large, it is still possible that the highly anisotropic shape of the cluster and the deformed bonds generate an anisotropy that is larger than or comparable to the observed Kondo temperature,  $T_K \sim 70$  K. The effect of anisotropy on the behavior of the grain is rather complex, and we

shall discuss it in a subsequent publication.<sup>31</sup> We would like to mention, however, two important results that may be relevant to the experiments. Large spin anisotropy is usually unfavorable to the Kondo effect. In most cases it leads to an Ising-like behavior with exponentially suppressed effective Kondo couplings, and gives rise to a dramatic decrease of  $T_K$ . However, for very small grains with a half-integer total spin and an almost perfect *planar* anisotropy, it can result in an effective strongly anisotropic Kondo coupling that is considerably *larger* than the couplings in Eq. (34). We find that for the smallest grains in Ref. 7 strong planar anisotropy could give rise to a  $T_K$  in the experimental range.

(e) Another possible source of error is our assumption that the calculated bulk density of states can be used for a small cluster. If the peak in the density of singly occupied states is shifted significantly from the energy value shown in Ref. 20, the value of  $J^{\text{eff}}$  might be increased. It is also possible that many-body corrections, omitted from our mean field model, could increase the value of  $J^{\text{eff}}$  sufficiently to account for the discrepancy with the experimental  $T_K$ .

It is interesting to compare the results for ferromagnetic Co clusters with nonmagnetic Ag clusters studied on single-wall metallic nanotubes.<sup>7</sup> The Ag clusters showed no Coulomb gap or discrete level spacing in the STM spectrum. This suggests that the Ag clusters were not in the weak tunneling regime where valence fluctuations can be ignored, and where an effective Kondo Hamiltonian can be derived for a particle with an odd number of electrons. (Indeed, if the coupling to the substrate is sufficiently large, the mean number of electrons on the cluster may be far from an integer, and the distinction between even and odd becomes meaningless.) Our analysis suggests that a Kondo effect can occur for a particle of a nonmagnetic metal, with odd electron number, if the coupling to the nanotube is in an appropriate intermediate regime.

It is also interesting to compare the results for Co particles on nanotubes with measurements of several Co particles on a highly-oriented pyrolytic graphite (HOPG) sheet reported in Ref. 7. The STM measurements did not show apparent single-particle levels in the latter case. Assuming that the coupling to a nanotube and graphite were not too different, this could be explained by a higher density of states on the HOPG surface.<sup>32</sup> (Recall that for 1 nm Co clusters on nanotubes, the level broadening was roughly equal to the level spacing. Thus the levels may be broadened beyond resolution on the HOPG surface.) The STM measurements typically show a minimum in the  $dI/dV$  spectrum near zero bias, when tunneling into the Co cluster on HOPG, but the width of the feature is relatively large. When fit to a Fano formula for a Kondo resonance, the authors of Ref. 7 obtained values of  $T_K$  of order 700 K even for clusters as large as 1 nm in diameter. Since it was not possible to raise the temperature enough to observe a temperature effect on the tunneling feature, however, supporting evidence for existence of a Kondo effect could not be obtained from this source. We note that STM measurements for tunneling directly into the HOPG substrate also show a minimum at zero bias.

Differences in the coupling of Co clusters to a nanotube or graphite surface may also play a role in the observed

spectral differences. Theoretical and experimental studies of STM images of graphite surfaces have indicated that there is an asymmetry in the local density of states at nearest-neighbor atoms.<sup>33</sup> This difference may also play a role in the interpretation of the spectra of Co on HOPG. Finally, it is possible that the matrix element for coupling between the cluster and the nanotube is reduced relative to the coupling to graphite due to the curvature of the nanotube.

## VII. CONCLUSIONS

In this paper we have studied electron scattering from ferromagnetic clusters on a metallic substrate. We studied two cluster models. The first model describes itinerant ferromagnetism<sup>11</sup> and is probably appropriate for the description of experiments such as those of Odom *et al.*<sup>7</sup> on Co clusters. We also proposed another solvable cluster model, where spins on the  $d$  levels are treated as *localized* entities. This latter model may be more appropriate for nanoscale rare-earth ferromagnets or semiconducting ferromagnets such as GaMnAs, though in both cases spin-orbit interaction plays an important role and leads to strong spin-anisotropy effects.

We derived a general expression for the Kondo couplings  $J^{\mu\nu}$  for both ferromagnetic cluster models. The sign of the obtained coupling depends in both models on the details of the band structure. For the itinerant model, virtual tunneling onto the singly occupied levels on the cluster induces an antiferromagnetic exchange interaction, while doubly occupied and unoccupied levels generate a ferromagnetic contribution to the exchange coupling.

We have shown that for Co clusters the itinerant model leads to *dominantly antiferromagnetic coupling* between the cluster spin and the conduction electron spins. However, fluctuations to doubly occupied and empty states give a large ferromagnetic contribution to the exchange coupling that reduce it to roughly half its original value, and thus cannot be neglected. (As we discussed in Sec. III, for the nonferromagnetic spin  $S=1$  islands studied in Ref. 23 these ferromagnetic contributions are small.)

The exchange coupling  $J^{\mu\nu}$  involves various scattering channels. Therefore, in principle, the cluster could produce a series of Kondo effects where the spin of the cluster is gradually screened.<sup>25</sup>

It is important to emphasize that in the regime of weak electron tunneling between the metallic substrate and the cluster, ferromagnetism has no special role in producing the Kondo effect as we have emphasized in Sec. IV B. In fact, our calculation shows that ferromagnetism tends to *suppress the Kondo temperature with increasing  $N_A$  more so than for the case of a non-ferromagnetic cluster*. Besides the “strength” of the ferromagnetism,  $U$ , the Kondo scale is also affected by the density of states on the cluster and finite charging energy, as well as the cluster-metal conductance.

The weak tunneling analysis we performed is only appropriate if the conductance between the cluster and the metal lead is smaller than the quantum conductance. Increasing the number of tunneling points leads to an increase in the cluster-metal conductance. Once this conductance becomes

larger than the quantum conductance, the effective charging energy is renormalized to a value close to zero, and a perturbative computation in  $\hat{V}$  breaks down. In this regime extended states on the cluster are strongly hybridized with those in the metal, and can be viewed as part of the extended states in the metal.

In the regime of strong electron tunneling between the substrate and cluster, it is not clear whether the itinerant model is able to produce a Kondo effect. On the other hand, our local moment cluster model gives a natural description of the strong tunneling regime. In the local moment model the localized  $d$ -electron spins can be viewed as a magnetic cluster embedded in the metallic host. This model has been analyzed in detail in Ref. 24. In our local moment model, antiferromagnetic exchange [ $J>0$  in Eq. (35)] between the local moments and the conduction electrons produces a Kondo effect in the strong tunneling regime, though, the Kondo temperature decreases very fast with increasing cluster size. We have also argued that within the local moment model, the effective coupling between the electrons in the substrate and the cluster spin must change sign as one gradually increases the tunneling between the cluster and the substrate.

Both the itinerant and local moment calculations show that the Kondo coupling is *inversely* proportional to the *total spin*  $S_T$  of a ferromagnetic cluster, which in turn, is proportional to the size of the cluster.<sup>34</sup> The Kondo effect is due to quantum fluctuations of the cluster spin, and these are suppressed as  $1/S_T$  for large ferromagnetic clusters. Thus  $T_K$  goes to zero *exponentially* with increasing cluster size.

To make stronger contact with the experiments of Ref. 7 on Co clusters on a carbon nanotube, we also calculated the STM spectra of a ferromagnetic cluster as described in Sec. IV A. We found that mesoscopic fluctuations in the charging energies may give rise to interesting qualitative changes and asymmetries in the STM spectrum. It is possible, for example, that the positively and negatively charged states of the cluster have very different decay rates and therefore the positive (negative) voltage side of the spectrum shows discrete levels while the negative (positive) voltage side displays a continuum spectrum.

We can use the model parameters extracted from the high-energy part of the STM spectra to make an estimate of  $T_K$  and predict how it scales with cluster size. Our results agree with the experiments in that they produce a rapid decrease of  $T_K$  thereby rendering the Kondo effect impossible to observe in larger clusters. However, the Kondo temperature we find is already too small by a factor of  $\sim 500$  compared to the  $T_K$  observed for a small cluster of  $\sim 8$  atoms. In Sec. VI we have enumerated a number of effects which might raise  $T_K$  relative to the predictions of our simple model which may be a possible explanation for the discrepancy between theory and experiment. We remark that by neglecting the ferromagnetic contributions to the exchange coupling one would obtain a  $T_K$  that is larger by a factor of  $\sim 10^3$ . Thus the ferromagnetic contributions to the effective coupling are essential and cannot be neglected.

Many open questions remain regarding the physics of small ferromagnetic clusters. Among them are: (i) accurate estimates of the net spin of 5–50 atom clusters supported on

a substrate; (ii) Magnetic anisotropy energies in clusters of this size; (iii) the nature of nonequilibrium and other many body effects. We believe that the STM is a crucial tool for gathering cluster-specific data for ferromagnetic nanoparticles and will undoubtedly reveal even more intriguing physics of these tiny systems in the years to come.

### ACKNOWLEDGMENTS

We are very grateful to T. Odom and C.M. Lieber for many discussions on their experiments and for sharing their data prior to publication and to A.H. Castro Neto, Jan von Delft, and M. Pustilnik for useful discussions. This research was supported by ITAMP, DIP Grant No. c-7.1, ISF Grant No. 160/01-1, NSF Grants Nos. DMR 98-09363, DMR 99-81283, and DMR-97-14725, and Hungarian Grants Nos. OTKA F030041, T029813, and 29236.

### APPENDIX A: DERIVATION OF THE LOCAL MOMENT MODEL

Consider  $N_A$  magnetic impurities embedded in close proximity in a metallic host. The Hamiltonian is  $\hat{H} = \hat{H}_{\text{metal}} + \hat{H}_{\text{int}}$  where  $\hat{H}_{\text{metal}} = \sum_{\mu,k,\sigma} \epsilon_{\mu,k} \hat{n}_{\mu k \sigma}$  describes the free conduction electrons and

$$\hat{H}_{\text{int}} = - \sum_{\vec{r}, \vec{r}'} J_F(\vec{r}, \vec{r}') \vec{S}_d(\vec{r}) \cdot \vec{S}_d(\vec{r}') + J \sum_r \vec{S}_c(\vec{r}) \cdot \vec{S}_d(\vec{r}) \quad (\text{A1})$$

describes the direct interactions between the impurity  $d$  levels and the interactions between the conduction electrons and the magnetic impurities. The first term in Eq. (A1) describes the ferromagnetic interaction among the localized  $d$  levels of the impurity atoms and the second term,  $H_K \equiv J \sum_r \vec{S}_c(\vec{r}) \cdot \vec{S}_d(\vec{r})$ , describes Kondo scattering from these  $d$  levels by the conduction electrons.  $J_F(\vec{r}, \vec{r}') > 0$  is the ferromagnetic exchange interaction between two localized  $d$ -levels and  $J > 0$  is the bare Kondo exchange coupling between the  $d$  levels and the conduction electrons. The conduction-electron spin operator at position  $\vec{r}$  is

$$\vec{S}_c(\vec{r}) = \frac{1}{2} \sum_{j,j'} \varphi_j^*(\vec{r}) \varphi_{j'}(\vec{r}) c_{j\alpha}^\dagger \vec{\sigma}_{\alpha\alpha'} c_{j'\alpha'}, \quad (\text{A2})$$

where  $\varphi_j(\vec{r})$  is the wave function of conduction electrons with level index  $j$  at  $\vec{r}$ . The utility of Eq. (A1) is twofold.

(i) It gives an expression for the important limiting case of a ‘‘cluster’’ which consists of just one impurity. In this limit,  $\hat{H}_{\text{int}} = J \vec{S}_c(0) \cdot \vec{S}_d(0)$  which is just  $H_K$  for a single impurity.

(ii) Equation (A1) can describe the limit of a cluster so strongly coupled to the metallic host that the conduction-band conduction electrons of the cluster and those of the host cannot be distinguished.

Thus, the character of the  $\varphi_j(\vec{r})$  that appear in Eq (A2) varies depending on the physical situation. For a single impurity,  $\varphi_j(\vec{r})$  is the wave function of the host metal conduction electrons, for a cluster in the weak tunneling regime as

described in Sec. III  $\varphi_j(\vec{r})$  describes the conduction-band wave functions of the ferromagnet or ferromagnetic semiconductor and for a cluster in the strong tunneling regime  $\varphi_j(\vec{r})$  is a strong hybridization of the ferromagnetic conduction-band electrons and the conduction electrons of the host metal.

To derive Eq. (35), we neglect anisotropy in the cluster magnetization formed by the localized  $d$  levels. We further neglect spin-wave excitations to states of different total  $d$  electron spin of the cluster. In a Heisenberg-type model one may estimate the cost for such an excitation as  $E_{\text{spin-wave}} \sim J_F(ak)^2$  where  $a$  is the lattice spacing of the cluster’s atoms and  $k$  is the largest wave vector of the spin wave allowed by the physical size of the cluster. If we take  $J_F \sim 0.1$  eV, e.g., then for a small cluster of size  $L \sim 10$  Å with lattice constant  $a \sim 2.5$  Å,  $k_{\text{min}} \sim \pi/L$  so that the minimum spin-wave energy  $E_{\text{spin-wave}}^{\text{min}} \sim 60$  meV  $\approx 600$  K. Below that energy scale spin waves can be therefore neglected and we can concentrate on the subspace where

$$\sum_r \vec{S}_d(\vec{r}) = N_A S_d = S_d^{\text{max}}. \quad (\text{A3})$$

Within the subspace of maximum total  $d$  level spin, the  $d$  level spin is a rigid spin which can only change its projection on the  $z$  axis. The collective effect of the impurity  $d$  levels is to give the cluster a net spin. It is this spin that conduction electrons will scatter from—either ‘‘directly’’ in the limit of strong tunneling between the cluster and metallic host or ‘‘indirectly’’ as described in Sec. III in the limit of weak tunneling. (In the limit of weak tunneling only conduction-band electrons may hop on and off the cluster.) Within the  $S_d = S_d^{\text{max}}$  subspace,

$$\begin{aligned} \langle S_d, S_d^z | \hat{H}_K | S_d, S_d^z \rangle \\ = \frac{J}{2} \sum_{r,j,j'} \varphi_j^*(\vec{r}) \varphi_{j'}(\vec{r}) c_{j\alpha}^\dagger \vec{\sigma}_{\alpha\alpha'} c_{j'\alpha} \langle S_d, S_d^z | \vec{S}_d(\vec{r}) | S_d, S_d^z \rangle \end{aligned} \quad (\text{A4})$$

$$\begin{aligned} \approx \frac{J}{2} \sum_{r,j,j'} \varphi_j^*(\vec{r}) \varphi_{j'}(\vec{r}) c_{j\alpha}^\dagger \vec{\sigma}_{\alpha\alpha'} c_{j'\alpha} \\ \times \frac{1}{N_A} \langle S_d, S_d^z | \vec{S}_d | S_d, S_d^z \rangle. \end{aligned} \quad (\text{A5})$$

The sum over  $\vec{r}$  can be estimated,

$$\sum_r \varphi_j^*(\vec{r}) \varphi_{j'}(\vec{r}) = \begin{cases} 1 & j = j' \text{ (normalization)} \\ \sim \frac{1}{\sqrt{N_A}} & j \neq j' \text{ (random numbers)} \end{cases} \quad (\text{A6})$$

Neglecting the off-diagonal terms,

$$H_K \approx \frac{J}{N_A} \frac{1}{2} \sum_j c_{j\alpha}^\dagger \vec{\sigma}_{\alpha\alpha'} c_{j'\alpha} \cdot \vec{S}_d \quad (\text{A7})$$

$$= \frac{J}{N_A} \vec{S}_c \cdot \vec{S}_d \quad (\text{A8})$$

The full Hamiltonian is

$$H_{\text{cluster}} = \sum_{j,\sigma} \epsilon_j \hat{n}_{j\sigma} + \frac{J}{N_A} \vec{S}_c \cdot \vec{S}_d + \frac{E_C}{2} \left( \sum_{j,\sigma} \hat{n}_{j\sigma} - n_g \right)^2 - \sum_{\vec{r},\vec{r}'} J_F(\vec{r},\vec{r}') \vec{S}_d(\vec{r}) \cdot \vec{S}_d(\vec{r}') \quad (\text{A9})$$

where we have put in the Coulomb charging energy by hand. Recall that now the  $c_{j\sigma}^\dagger$  refer to conduction-band electrons, not  $s$ ,  $p$ , and  $d$  hybridized bands as in the itinerant model. The last term in Eq. (A9) is just an irrelevant shift in the total energy in the subspace  $S_d = S_d^{\text{max}}$  so we drop it. Thus, we arrive at

$$\hat{H}_{\text{cluster}} = \sum_{j,\sigma} \epsilon_j \hat{n}_{j\sigma} + \frac{J}{N_A} \vec{S}_c \cdot \vec{S}_d + \frac{E_C}{2} \left( \sum_{j,\sigma} \hat{n}_{j\sigma} - n_g \right)^2. \quad (\text{A10})$$

## APPENDIX B: MATRIX ELEMENTS AND KONDO COUPLINGS FOR THE LOCAL MOMENT MODEL

In this Appendix, we include some more lengthy expressions not included in Sec. V B. To complete the evaluation the RHS of Eq. (19) for the local moment model described in Sec. V B we need the matrix elements,

$$M_2 \equiv {}^N \langle S_T, S_T - 1 | c_{j\uparrow} | S_T + 1/2, S_T - 1/2 \rangle_j^{N+1} = - \sum_{S_c^z = -S_c}^{S_c} \sqrt{\frac{S_c - S_c^z}{2S_c}} \langle S_c, S_d; S_c^z, S_T - S_c^z - 1 | S_T, S_T - 1 \rangle \times \langle S_c - 1/2, S_d; S_c^z + 1/2, S_T - S_c^z - 1 | S_T + 1/2, S_T - 1/2 \rangle, \quad (\text{B1})$$

$$M_3 \equiv {}^{N-1} \langle S_T + 1/2, S_T - 1/2 | c_{j\uparrow} | S_T, S_T \rangle^N = \sum_{S_c^z = -S_c}^{S_c} \sqrt{\frac{S_c + S_c^z}{2S_c}} \langle S_c, S_d; S_c^z, S_T - S_c^z | S_T, S_T \rangle \times \langle S_c - 1/2, S_d; S_c^z - 1/2, S_T - S_c^z | S_T + 1/2, S_T - 1/2 \rangle, \quad (\text{B2})$$

$$M_4 \equiv {}^N \langle S_T, S_T - 1 | c_{j\downarrow}^\dagger | S_T + 1/2, S_T - 1/2 \rangle_j^{N-1} = \sum_{S_c^z = -S_c}^{S_c} \sqrt{\frac{S_c - S_c^z}{2S_c}} \langle S_c, S_d; S_c^z, S_T - S_c^z - 1 | S_T, S_T - 1 \rangle \times \langle S_c - 1/2, S_d; S_c^z + 1/2, S_T - S_c^z - 1 | S_T + 1/2, S_T - 1/2 \rangle. \quad (\text{B3})$$

The matrix elements then directly yield the expression for the generalized Kondo couplings for the local moment model,

$$\tilde{J}_s^{\mu\nu} = \sqrt{\frac{2}{S_T j + 1}} \sum_{\mu}^A V_{\mu}^{j,k_f*} V_{\nu}^{j,k_i} \times \left( \frac{M_4 M_3}{\delta E_{-, \uparrow} + \epsilon_A - \epsilon_j} - \frac{M_2 M_1}{\delta E_{+, \uparrow} - \epsilon_{l+1} + \epsilon_j} \right), \quad (\text{B4})$$

where  $M_1$  denotes the matrix element already given in Eq. (40). The products  $M_4 M_3$  and  $M_2 M_1$  can be evaluated directly,

$$\tilde{J}_s^{\mu\nu} = - \frac{1}{S_T + 1} \sum_{j=l+1}^A V_{\mu}^{j,k_f*} V_{\nu}^{j,k_i} \times \left( \frac{1}{\delta E_{-, \uparrow} + \epsilon_A - \epsilon_j} + \frac{1}{\delta E_{+, \uparrow} - \epsilon_{l+1} + \epsilon_j} \right), \quad (\text{B5})$$

giving a ferromagnetic contribution when  $J > 0$ . If  $J < 0$  and  $S_T = S_d + S_c$  ( $\uparrow \rightarrow \downarrow$ ) one finds  $-1/(S_T + 1) \rightarrow 1/(S_T)$ , which agrees with Eq. (23) of the itinerant model with  $S_T \rightarrow S_0$ .

A calculation similar to the one that led to Eq. (B4) and Eq. (B5) then yields:

$$\tilde{J}_e^{\mu\nu} = \sum_{j>A} V_{\mu}^{j,k_f*} V_{\nu}^{j,k_i} \times \left( \frac{2}{2S_T + 1} - \frac{1}{S_T + 1} \left( \frac{2S_c}{2S_c + 1} \right) \right) \times \left( \frac{1}{\delta E_{+, \downarrow} - \epsilon_{A+1} + \epsilon_j} - \frac{1}{\delta E_{+, \uparrow} + \Delta_s - \epsilon_{A+1} + \epsilon_j} \right), \quad (\text{B6})$$

and from the doubly occupied states

$$\tilde{J}_d^{\mu\nu} = \sum_{j<=l} V_{\mu}^{j,k_f*} V_{\nu}^{j,k_i} \times \left( \frac{2}{2S_T + 1} - \frac{1}{S_T + 1} \left( \frac{2S_c}{2S_c + 1} \right) \right) \times \left( \frac{1}{\delta E_{-, \downarrow} + \epsilon_l - \epsilon_j} - \frac{1}{\delta E_{-, \uparrow} + \Delta_s + \epsilon_l - \epsilon_j} \right), \quad (\text{B7})$$

where we have again assumed  $J > 0$ , giving  $\tilde{J}_e^{\mu\nu} > 0$  and  $\tilde{J}_d^{\mu\nu} > 0$  since  $\delta E_{\pm, \sigma} \sim E_C/2$ . In the limit of a single point of contact, one recovers an expression similar to Eq. (26), Eq. (41), except with an overall sign difference when  $J > 0$  (and the precise form of the mesoscopic fluctuations). In the case  $J < 0$  (take  $\uparrow \rightarrow \downarrow$  and  $\downarrow \rightarrow \uparrow$ ) we have

$$\frac{2}{2S_T + 1} \rightarrow - \frac{2}{2S_T + 1}$$

and

$$\frac{1}{S_T + 1} \left( \frac{2S_c}{2S_c + 1} \right) \rightarrow - \frac{1}{S_T} \left( \frac{2S_c}{2S_c + 1} \right)$$

which makes  $\tilde{J}_e^{\mu\nu} < 0$  and  $\tilde{J}_d^{\mu\nu} < 0$ .

The reduced matrix elements<sup>35</sup> for all the states of the local moment model are given below.

(1)  $J > 0$ ,

$${}_j^{N-1}\langle S_T+1/2||c_j||S_T\rangle_d^N = \sqrt{\frac{2S_c}{2S_c+1}}\sqrt{2S_T+2},$$

$${}_j^{N-1}\langle S_T+1/2||c_j||S_T\rangle_d^N = \frac{2S_T+2}{\sqrt{2S_T+1}},$$

$${}_j^{N-1}\langle S_T-1/2||c_j||S_T\rangle_d^N = \frac{2S_T}{\sqrt{2S_T+1}},$$

$${}_j^{N-1}\langle S_T-1/2||c_j||S_T\rangle_d^N = \sqrt{2S_T}\sqrt{\frac{2S_c}{2S_c+1}},$$

$${}_j^{N+1}\langle S_T+1/2||c_j^\dagger||S_T\rangle_s^N = \frac{2S_T+1}{\sqrt{2S_T+2}},$$

$${}_j^{N+1}\langle S_T-1/2||c_j^\dagger||S_T\rangle_s^N = \frac{2S_T+1}{\sqrt{2S_T}},$$

$${}_j^{N-1}\langle S_T+1/2||c_j||S_T\rangle_s^N = \sqrt{2S_T+2},$$

$${}_j^{N-1}\langle S_T-1/2||c_j||S_T\rangle_s^N = \sqrt{2S_T},$$

$${}_j^{N+1}\langle S_T+1/2||c_j^\dagger||S_T\rangle_e^N = \frac{2S_T+1}{\sqrt{2S_T+2}}\sqrt{\frac{2S_c}{2S_c+1}},$$

$${}_j^{N+1}\langle S_T+1/2||c_j^\dagger||S_T\rangle_e^N = \sqrt{2S_T+1},$$

$${}_j^{N+1}\langle S_T-1/2||c_j^\dagger||S_T\rangle_e^N = \sqrt{2S_T+1}.$$

$${}_j^{N+1}\langle S_T-1/2||c_j^\dagger||S_T\rangle_e^N = \frac{2S_T+1}{\sqrt{2S_T}}\sqrt{\frac{2S_c}{2S_c+1}}.$$

(2)  $J < 0$

<sup>1</sup>A.C. Hewson, *The Kondo Problem to Heavy Fermions* (Cambridge University Press, Cambridge, England, 1997).

<sup>2</sup>D. Goldhaber-Gordon, H. Shtrikman, D. Mahalu, D. Abusch-Magder, U. Meirav, and M.A. Kastner, *Nature (London)* **391**, 156 (1998); D. Goldhaber-Gordon, J. Göres, M.A. Kaster, H. Shtrikman, D. Mahalu, and U. Meirav, *Phys. Rev. Lett.* **81**, 5225 (1998).

<sup>3</sup>S. Sasaki, S. De Franceschi, J.M. Elzerman, W.G. van der Wiel, M. Eto, S. Tarucha, and L.P. Kouwenhoven, *Nature (London)* **405**, 764 (2000); W.G. van der Wiel, S. De Franceschi, T. Fujisawa, J.M. Elzerman, S. Tarucha, and L.P. Kouwenhoven, *Science* **289**, 2105 (2000).

<sup>4</sup>J. Li, W-D. Schneider, R. Berndt, and B. Delley, *Phys. Rev. Lett.* **80**, 2893 (1998); V. Madhavan, W. Chen, T. Jamneala, M.F. Crommie, and N.S. Wingreen, *Science* **280**, 567 (1998); T. Jamneala, V. Madhavan, W. Chen, and M.F. Crommie, *Phys. Rev. B* **61**, 9990 (2000).

<sup>5</sup>H.C. Manoharan, C.P. Lutz, and D.M. Eigler, *Nature (London)* **403**, 512 (2000).

<sup>6</sup>J. Nygard, D.H. Cobden, and P.E. Lindelof, *Nature (London)* **408**, 342 (2000).

<sup>7</sup>T.W. Odom, J-L. Huang, C.L. Cheungm, and C.M. Lieber, *Science* **290**, 1549 (2000); T.W. Odom, Ph.D. thesis, Harvard University, 2000.

<sup>8</sup>As far as we are aware, no STM experiments on metallic nanotubes supported on metallic substrates have shown evidence of Luttinger-liquid effects in the tunneling spectrum, perhaps due to charge screening by the substrate. We therefore neglect electron-electron interactions in our model of the nanotube conduction electrons. [Transport measurements on ropes of SWNT supported on an insulating substrate have, however, shown Luttinger-Liquid behavior: M. Bockrath, D.H. Cobden, J. Lu, A.G. Rinzler, R.E. Smalley, L. Balents, and P.L. McEuen, *Nature (London)* **397**, 598 (1999)].

<sup>9</sup>In the experiments with magnetic atoms adsorbed on metallic surfaces like those described in Refs. 4 and 5 a diplike feature

was typically observed rather than a peak. The  $dI/dV$  vs  $V$  line shape depends sensitively on the details of the impurity–conduction electron coupling and STM tip location. For a discussion see: M. Plihal and J.W. Gadzuk, *Phys. Rev. B* **63**, 085404 (2001); A. Schiller and S. Hershfield, *Phys. Rev. B* **61**, 9036 (2000) and Ref. 10.

<sup>10</sup>O. Újsághy, J. Kroha, L. Szunyogh, and A. Zawadowski, *Phys. Rev. Lett.* **85**, 2557 (2000).

<sup>11</sup>C.M. Canali and A.H. MacDonald, *Phys. Rev. Lett.* **85**, 5623 (2000).

<sup>12</sup>S. Kleff, J. von Delft, M.M. Deshmukh, and D.C. Ralph, *Phys. Rev. B* **64**, 220401 (2001).

<sup>13</sup>H. Ohno, *Science* **281**, 951 (1998).

<sup>14</sup>R. Saito, G. Dresselhaus, and M.S. Dresselhaus, *Physical Properties of Carbon Nanotubes* (Imperial College Press, London, 1998).

<sup>15</sup>P. Nozieres and A. Blandin, *J. Phys. (France)* **41**, 193 (1980).

<sup>16</sup>O. Újsághy, A. Zawadowski, and B.L. Gyroffly, *Phys. Rev. Lett.* **76**, 2378 (1996); O. Újsághy and A. Zawadowski, *Phys. Rev. B* **57**, 11 598 (1998); **57**, 11 609 (1998).

<sup>17</sup>S. Guéron, M.M. Deshmukh, E.B. Myers, and D.C. Ralph, *Phys. Rev. Lett.* **83**, 4148 (1999); M.M. Deshmukh, S. Kelff, S. Guéron, E. Bonet, A.N. Pasupathy, J. von Delft, and D.C. Ralph, *ibid.* **87**, 226801 (2001).

<sup>18</sup>In a semiconductor quantum dots (Refs. 2,3) and nanotube quantum dots (Ref. 6)  $n_g$  can be tuned by a variable external gate voltage, thereby controlling the equilibrium number of electrons on the dot (cluster). For a ferromagnetic cluster adsorbed on a metallic surface,  $n_g$  is set by the chemistry of the cluster-metal interface and can not be freely changed in an experiment.

<sup>19</sup>The itinerant model presented has a  $(2S_0+1)$ -fold degeneracy. In a real ferromagnetic cluster there will be anisotropy which, in the simplest case, will appear as a uniaxial anisotropy (Ref. 12). For Co, the anisotropy energy can be estimated to be of the order (Ref. 12)  $0.01-0.1$  meV  $\approx 0.1-1.0$  K, which is safely below the

- experimental temperature range of 4–100 K (Ref. 7), so we ignore it.
- <sup>20</sup>D.A. Papaconstantopoloulos, *Handbook of the Band Structure of Elemental Solids* (Plenum, New York, 1986).
- <sup>21</sup>This definition is only appropriate for a partially polarized conduction band. If  $U$  is large enough to fully polarize the bands a more appropriate definition could be the energy difference of the highest occupied spin-up level and that of the lowest *empty* spin-down level. In this case the particle-hole excitation energy can clearly be substantially larger than the single-particle level spacing and be of the order of the band splitting.
- <sup>22</sup>An alternative proof was given independently for the special case of a  $2 \times 2J^{\mu\nu}$  in Ref. 22.
- <sup>23</sup>M. Pustilnik and L.I. Glazman, Phys. Rev. Lett. **87**, 216601 (2001).
- <sup>24</sup>K. Levin and D.L. Mills, Phys. Rev. B **9**, 2354 (1974).
- <sup>25</sup>W.G. van der Wiel, S. De Franceschi, J.M. Elzerman, S. Tarucha, L.P. Kouwenhoven, J. Motohisa, F. Nakajima, and T. Fukui, Phys. Rev. Lett. **88**, 126803 (2002).
- <sup>26</sup>J. Tersoff and D.R. Hamann, Phys. Rev. Lett. **50**, 1998 (1983).
- <sup>27</sup>Using the experimentally observed level widths of the Co clusters on nanotubes (Ref. 7) and the density of states of a metallic nanotube (Ref. 14) we estimate the bare hopping element (overlap integral) in a tight-binding model from an atom of the nanotube to the nearest Co cluster atom to be  $\sim 3\text{--}4$  eV. This is comparable to the overlap integral of the nearest-neighbor C-C overlap integral in nanotubes, 2.5 eV (Ref. 14).
- <sup>28</sup>I.L. Aleiner, B.L. Altshuler, Y.M. Galperin, and T.A. Shutenko, Phys. Rev. Lett. **86**, 2629 (2001).
- <sup>29</sup>K. Yamada, K. Yoshida, and K. Hansawa, Prog. Theor. Phys. **71**, 450 (1984).
- <sup>30</sup>F.J. Himpsel, J.E. Ortega, G.J. Mankey, and R.F. Willis, Adv. Phys. **47**, 511 (1998).
- <sup>31</sup>G. A. Fiete, G. Zarand, and B. I. Halperin (unpublished).
- <sup>32</sup>We may compare the density of states/atom of a nanotube to that of bulk graphite. The density of states of bulk graphite was obtained from the expanded (unlabeled) version of Eq. (5.4) in P.R. Wallace, Phys. Rev. **71**, 622 (1947) with  $\gamma_1 = .6$  eV (Ref. 33) and  $\gamma_0 = 3.13$  eV for 3D graphite from 810 of Ref. 14 where  $\gamma_0$  is the nearest-neighbor tight-binding hopping energy *in plane* and  $\gamma_1$  is the hopping energy between nearest neighbors *between planes*. For the density of states of the nanotube, we use Eq. (19.32) of Ref. 14 with  $\gamma_0 = 2.5$  eV for 2D graphite. Note that in this case  $\gamma_0$  is slightly lower than the 3D value due to averaging of the asymmetry of the bonding and antibonding states. The final values we obtain are  $\rho_{\text{graphite}}(E_F) = 0.023$  eV/atom and for a 1 nm nanotube  $\rho_{\text{nanotube}}(E_F) = 0.014$  eV/atom.
- <sup>33</sup>D. Tomanek, S.G. Louie, H.J. Mamin, D.W. Abraham, R.E. Thomson, E. Ganz, and J. Clarke, Phys. Rev. B **35**, 7790 (1987); D. Tomanek and S.G. Louie, *ibid.* **37**, 8327 (1988).
- <sup>34</sup>We assumed that the magnetization per atom on the cluster is independent of the size of the cluster.
- <sup>35</sup>We use the conventions of J.J. Sakurai, *Modern Quantum Mechanics Revised Edition* (Addison-Wesley, Massachusetts, 1994), p. 239.